Antiferromagnetic garnets

K. P. Belov and V. I. Sokolov

Moscow State University
Usp. Fiz. Nauk **121**, 285–317 (February 1977)

The authors consider the results of experimental investigations of garnets in which antiferromagnetic ordering occurs because of the weak exchange interaction within one of the sublattices: dodecahedral, octahedral, or tetrahedral. They discuss the characteristics of magnetic phase transitions in rare-earth gallates and aluminates, whose magnetic properties are described by the Ising model of an antiferromagnet with allowance for the effects of the crystalline field. They analyze the magnetic phase diagrams and critical behavior of garnets with rare-earth ions in dodecahedra. They describe the magnetic characteristics of garnets containing $3d$ ions and consider the peculiarities of their behavior in an octahedral crystalline field. Taking the magnetic structure into account, they analyze antiferromagnetic exchange interactions in the garnet structure and the results of experimental study of the specific heat and of antiferromagnetic resonance in the spin-flop state of garnets with magnetic ions in octahedra. It is shown that the magnetic properties of these compounds are well described in the molecular-field approximation. Finally, magnetic structures and exchange interactions are discussed for antiferromagnetic garnets whose tetrahedral sublattice is formed by Fe^{3+} ions.

PACS numbers: 75.30.Kz, 75.30.Et, 75.40.Dy, 75.50.Ee

CONTENTS

1. INTRODUCTION

Since the publication in the thirties of the theoretical papers of Néel[1] and of Landau,[2] in which a beginning was made in the study of antiferromagnetism, an enormous number of antiferromagnetic materials have been discovered and investigated. Their magnetic, optical, high-frequency, and other properties have been elucidated in detail in a number of monographs and reviews, including ones by Soviet authors.[3–7]

The present review has the purpose of acquainting the reader with investigations of a new, very numerous class of cubic antiferromagnets with the garnet structure. This structure received its name from the orthosilicate garnet minerals (for example, $Ca_3Al_2Si_3O_{12}$) and is described by the space group $Ia3d$–O_h^{10}.

Among magnetic crystals with the garnet structure, the most studied are the iron garnets, which have already found wide technical application. The elementary cell of an iron garnet contains eight formula units $Me_3Fe_5O_{12}$, where Me is an ion of yttrium or of a rare-earth element. The metallic ions occupy interstices of the oxygen lattice; there are interstices of three types: dodecahedral or c sites, octahedral a sites, and tetrahedral or d sites. The local symmetry at all these cation positions is noncubic. The symmetry of the dodecahedral sites is the orthorhombic D_2 (there are six types of sites, with different directions of the local axes). The octahedral sites are characterized by the trigonal symmetry C_3; there are two kinds of distorted octahedra, turned with respect to the crystallographic direction ⟨111⟩ through opposite angles $\pm\alpha$, $\alpha \approx 28°$. The tetrahedral sites have the symmetry S_4, with tetragonal axes along crystal directions ⟨100⟩, with respect to which the oxygen tetrahedra are wound through angles $\pm\beta$, $\beta \approx 16°$, producing two types of nonequivalent sites.

The distribution of cations among c, a, and d sites in the garnet structure is customarily indicated by wavy, square, and round brackets respectively. Then the formula of a rare-earth iron garnet is written in the form

$$\{R_3^{3+}\}\,[Fe_2^{3+}]\,(Fe_3^{3+})\,O_{12}.$$

To explain the observed magnetic properties of iron garnets, Néel[8] developed a three-sublattice model. The sublattices are formed by the magnetic moments of ions at c, a, and d sites. The strongest interaction is indirect exchange between sublattices a and d: [Fe]–O–(Fe). This interaction is antiferromagnetic; therefore the magnetic moments of sublattices a and d are always oriented antiparallel to each other. The Curie temperature, which is determined by the a–d interaction, is almost the same for all rare-earth iron garnets and is about 550 °K. Next in strength is the antiferromagnetic indirect exchange interaction {R}–O–(Fe), because of which the moments of the c and d sublattices set themselves antiparallel.

The indirect exchange interactions between ions within each of the sublattices are also antiferromagnetic, but they are considerably weaker and therefore do not pre-

vent parallel orientation of the magnetic moments of the ions of each of the sublattices. But if in a rare-earth iron garnet we "disconnect" any two magnetic sublattices by substitution of diamagnetic ions, then at sufficiently low temperatures antiferromagnetic ordering occurs. Since the unique features of the garnet structure that result from isomorphic replacement of atoms by other atoms make it possible to synthesize "single-sublattice" garnets with various $3d$ and $4f$ ions, the peculiarities of the electronic states of the magnetic ions and their interactions with the crystal field of the lattice produce, in antiferromagnetic garnets, a great variety of physical properties.

In the present review, an attempt is made to summarize the principal results of experimental investigations of garnets in which, so far, antiferromagnetic ordering has been detected that is caused by exchange interactions of magnetic ions within one of the sublattices—c, a, or d.

In the first chapter of the review, principal attention is paid to the peculiarities of magnetic phase transitions in rare-earth gallates and aluminates. Consideration is given to the metamagnetism and tricritical behavior of the Ising antiferromagnet $Dy_3Al_5O_{12}$; ordering of the "two-singlet antiferromagnets," aluminates of terbium and holmium; and the role of hyperfine interactions in the antiferromagnetism of gallates with $T_N \approx 0.2\,^\circ$K.

The second chapter is devoted to analysis of the exchange interactions of garnets in whose octahedral sublattices magnetic $3d$ ions are located. It is shown that the properties of these Heisenberg antiferromagnets are well described in the molecular-field approximation when allowance is made for the peculiarities of the interaction of the $3d$ ions with the octahedral crystalline field. Here also are presented data on the study of the magnetic properties of garnets with rare-earth ions in the octahedra.

The third chapter discusses the exchange bonds and magnetic structure of garnets whose tetrahedral sublattice is formed by Fe^{3+} ions, whereas the octahedral and dodecahedral sublattices contain various nonmagnetic ions. The magnetic atoms in these garnets are isolated from one another by at least two oxygen atoms, and exchange interactions through two or even three intermediate links play an essential role in the formation of an antiferromagnetic structure.

2. GARNETS CONTAINING MAGNETIC IONS IN THE DODECAHEDRA

Antiferromagnetic ordering in compounds with the garnet structure was first discovered in rare-earth gallates, $R_3Ga_5O_{12}$ (RGaG), and aluminates, $R_3Al_5O_{12}$ (RAlG). Their detailed investigation[9-12] was undertaken primarily for the purpose of obtaining additional information about the magnetism of the iron garnets isomorphic with them, $R_3Fe_5O_{12}$. But it was then established that the rare-earth gallates and aluminates have independent interest as antiferromagnets whose peculiarities and whose variety of properties are to a considerable degree determined by effects of the crystal field.

Crystal fields in the garnet structure exert a significant influence on the rare-earth ions. It is known that for rare-earth ions with an odd number of electrons, a crystal field lifts the degeneracy to such a degree that there remains only the twofold degeneracy required by Kramers's theorem; that is, the electronic levels will consist of $(J+\frac{1}{2})$ doublets. Such "Kramers" ions include Sm^{3+}, Dy^{3+}, Er^{3+}, and Yb^{3+}. For ions with an even number of electrons in the $4f$ shell (Tb^{3+}, Ho^{3+}, Eu^{3+}), the ground state is a singlet with zero moment. But often the two lowest levels differ little in energy and in many respects behave like a doublet.

Magnetic $3d$ ions that can enter dodecahedral sites include Fe^{2+} ions (the natural mineral almandite, $Fe_3^{2+}Al_2Si_3O_{12}$) and Mn^{2+} (the mineral spessartite, $Mn_3^{2+}Al_2Si_3O_{12}$), which reveal antiferromagnetic ordering at helium temperatures.

A. Magnetic properties and exchange interactions of rare-earth gallates and aluminates

Table I shows the antiferromagnetic ordering temperatures (T_N) and the constants in the Curie-Weiss law for the paramagnetic susceptibility, $\chi_m = C_m/T - \theta_p$, for garnets in which the ground state of the rare-earth ion is a Kramers doublet.

The last three columns of Table I give the values of the g factor along the three principal axes of the crystal, obtained from EPR data on the R^{3+} ions ($\leq 1\%$) in the diamagnetic matrix of yttrium gallates and aluminates. From Table I it is seen that the behavior of the rare-earth ion differs significantly in gallium and aluminum garnets. This cannot be explained solely by the difference of the lattice parameters of rare-earth gallates and aluminates. In fact, the molecular volume of DyAlG is 7% smaller than that of DyGaG,[18] and T_N is significantly higher for the dysprosium aluminate. But in the case of erbium garnets the situation is reversed: in ErAlG no ordering is observed down to $0.3\,^\circ$K, whereas in erbium gallate $T_N = 0.79\,^\circ$K.

The values of the g factors for rare-earth ions in dodecahedral sites of a garnet attest to the high anisotropy of the R^{3+} ions; in DyAlG the largest is g_z (parallel to one of the cube edges of the elementary cell), while in DyGaG the g factor along the axis Ox (at angle 45° to a cubic axis) dominates. Estimates[19] show that in DyAlG the magnetocrystalline anisotropy energy exceeds by a

TABLE I. Magnetic characteristics of garnets with Kramers rare-earth ions.[13-17]

Garnet	T_N, °K	θ_p, °K	C_m, cgs emu/mol	R^{3+} in YGa(Al)G (4.2 °K)		
				g_x	g_y	g_z
NdGaG	0.516	—	1.03	2.027	1.251	3.660
SmGaG	0.918	—	—	—	—	—
GdGaG	—	−2.3	7.82	$g = 1.992$		
DyGaG	0.37	−0.1	8.0	13.45	0.57	3.41
DyAlG	2.54	−2.9	12.67	0.73	0.40	18.2
ErGaG	0.789	—	8.85	3.185	3.183	12.6
ErAlG	—	−2.3	4.3	7.75	3.71	7.35
YbAlG	—	−0.139	1.1	3.84	3.74	2.59

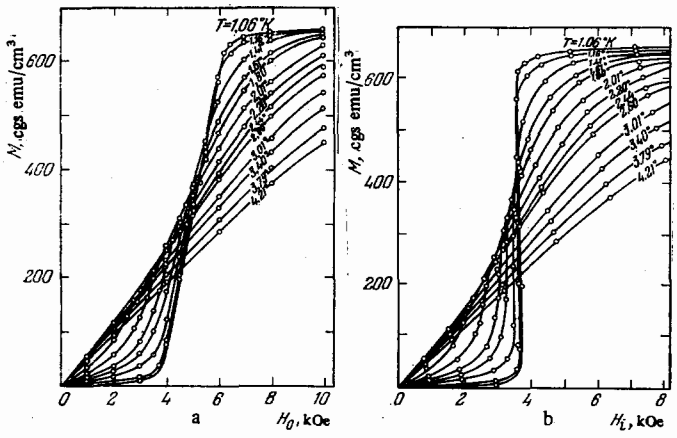

FIG. 1. Magnetization of a spherical DyAlG monocrystal near T_N, as a function (a) of the external field and (b) of the "true" field. Field applied along a [111] axis.

factor of almost 20 the interactions that cause antiferromagnetic ordering of this garnet at 2.5 °K. The exceptionally high local magnetic anisotropy alines the Dy^{3+} moments along one of the three crystal axes, so that the ordered state of DyAlG is a set of orthogonal pairs of sublattices parallel to $\pm X$, $\pm Y$, $\pm Z$.[17] In an external field $H_0 \parallel [111]$, these three directions become equivalent, and the system is well described by the Ising two-sublattice model. Below T_N this situation leads to the occurrence in DyAlG of a metamagnetic transition. Figure 1 shows isotherms of the magnetization along a [111] axis of a spherical specimen of DyAlG in the interval 1.06–4.21 °K.[19] Characteristic here is the existence in the field interval $4.0 \leq H_0 \leq 6.8$ kOe (Fig. 1a) of a transitional region, which the authors of[19] attribute to dipole interactions. Actually, the slope of the $M(H)$ curves in the transitional region is of order of magnitude $1/N$, where N is the demagnetizing factor. The dependence of the magnetization on the true field $H_i = H_0 - NM$ practically eliminates the transitional region (Fig. 1b), and here already $\partial M/\partial H_i \to \infty$; that is, a phase transition of the first kind occurs.

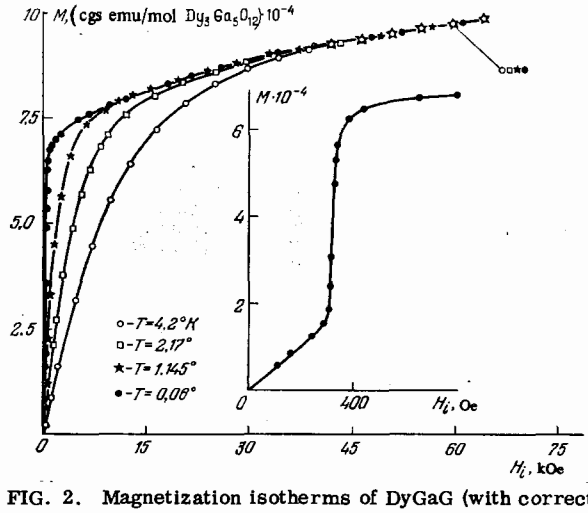

FIG. 2. Magnetization isotherms of DyGaG (with correction for the demagnetizing factor), for $H_i \parallel [100]$.

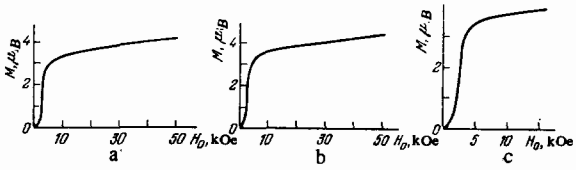

FIG. 3. Magnetization isotherms of ErGaG at $T = 0.08$ °K, along axes: (a), [001]; (b), [011]; (c) [111].

A metamagnetic behavior below T_N is observed also in the gallates of dysprosium[20] and erbium.[21] But as is seen from Fig. 2, which shows isotherms of the magnetization of DyGaG along a [100] axis in the temperature interval 0.06–4.2 °K, the threshold field in this specimen is almost an order of magnitude smaller than in DyAlG. It has been found[21] that the threshold fields for the three principal directions of an ErGaG crystal at $T = 0.08$ °K (Fig. 3) are close to the values given by a calculation according to the Ising model on the assumption of purely dipole interactions. The experimental values of the fields at which saturation magnetization is attained in directions [111], [110], and [100] exceed by about 10% the field values obtained from the calculation according to the Ising model. Furthermore, the shape of the magnetization curves of ErGaG and DyGaG differs from the corresponding curves for DyAlG. As is seen from Figs. 2 and 3, the erbium and dysprosium gallates show an appreciable susceptibility in the antiferromagnetic state and a quite gradual approach to saturation. It is assumed that these peculiarities are due to nonvanishing components of the g tensor ($g_x \approx g_y \approx 3.2$, $g_z = 12.6$ for ErGaG), whence the magnetic properties of ErGaG and DyGaG are not described exactly by the Ising model.

The Néel temperatures of garnets with the non-Kramers ions Tb^{3+} and Ho^{3+} are shown in Table II. Investigations of the magnetic properties have shown[22,23] that the terbium and holmium aluminates are characterized by metamagnetic behavior below T_N; the nature of the phase transition may change both with temperature (TbAlG) and also with the direction of the external magnetic field with respect to the crystal axes (HoAlG).

Figure 4 shows magnetization curves of TbAlG for various temperatures ($H_0 \parallel [111]$) according to the data of[22]. It is seen that above the critical temperature $T_{cr} = 0.71$ °K the metamagnetic transition in this garnet becomes a phase transition of the second kind. The experimentally observed threshold fields of the metamag-

TABLE II. Néel temperatures, magnitude of the singlet splitting (Δ), and saturation magnetic moment (m_s) for terbium and holmium garnets.[15,22–25]

Garnet	T_N, °K	Δ, °K	m_s, μ_B
TbAlG	1.35	2.5	7.6
TbGaG	0.25	2.87	6.68
HoAlG	0.86	4.66	8.2
HoGaG	0.19	7.40	7.69

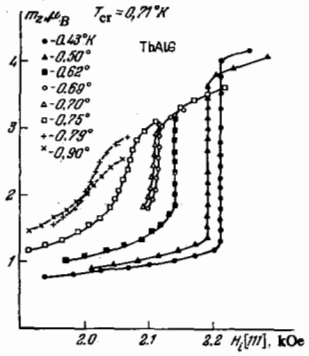

FIG. 4. Magnetization of a TbAlG monocrystal as a function of true field $\mathbf{H}_i \parallel [111]$,

netic transition (H_c) do not agree with the values of H_c calculated on the assumption that there is only dipole–dipole interaction. Allowance for exchange interaction improves the agreement with experiment (to with 5%). Thus for direction [111] in TbAlG one obtains

$$H_c^{exp} = (2220 \pm 10)\ \text{Oe}, \quad H_c^{dip} = 1405\ \text{Oe},$$

$$H_c^{dip+exch} = 2190\ \text{Oe}.$$

Ordering in rare-earth gallates and aluminates has been treated theoretically, by the molecular-field method, by Capel[26]; an analysis of exchange and dipole interactions in DyAlG has been given in[27,28]. On the basis of a Hamiltonian that takes account of dipole and exchange interactions and also of the effect of excited states (by means of the g tensor), Capel's theory makes it possible to determine the values of T_N and predicts three possible types of ordering of the rare-earth ions on the dodecahedral sublattice of the garnet: two antiferromagnetic (A and B) and a ferrimagnetic (C). The ordering temperatures according to Capel are calculated from dipole sums, exchange constants, (J_1, J_2, and J_3), and components of the g tensor. For DyAlG and ErGaG, quite good agreement is found between theoretical and experimental results: according to the theoretical calculations, these garnets have below T_N an antiferromagnetic structure of type A (magnetic moments of the sublattices parallel to the cubic axes of the crystal), and the theoretical values T_N^{theor}(ErGaG) = 0.82 °K and T_N^{theor}(DyAlG) = 2.52 °K are close to the experimental values given in Table I.

According to spectroscopic data,[29] the ground state of Tb^{3+} and Ho^{3+} in the aluminates is described by two singlets rather distant from the higher levels. For such a two-singlet antiferromagnet, a theory developed in[30] enables us to calculate, in the molecular-field approximation, the basic magnetic properties of TbAlG and HoAlG. The authors[30] showed that when the external magnetic field is applied along the [111] axis, TbAlG behaves like a two-sublattice antiferromagnet, for which the ordering temperature (T_N) is determined by the relation

$$\text{th}\left(\frac{\Delta}{2kT_N}\right) = \frac{\Delta}{2\gamma m_s^2}; \qquad (1)$$

here Δ is the energy of splitting of the fundamental doublet (values of Δ are given in Table II), γ is the molecular-field constant, calculated with allowance for dipole interactions only ($H_z^{eff} = \gamma m_z$), and m_s is the saturation magnetic moment (the nonvanishing component of magnetic moment between the two singlets). From the relation (1) it follows that the condition for existence of magnetic ordering is

$$\frac{\Delta}{2\gamma m_s^2} < 1. \qquad (2)$$

We note that for DyAlG (the ground state of Dy^{3+} is a doublet) the ordering temperature is determined[31] by the relation

$$4kT_N = \gamma\mu_B^2 g_z^2. \qquad (3)$$

Equations (1) and (3) coincide when $\Delta \to 0$; that is, TbAlG is a two-singlet analog of DyAlG. Thus the effect of Δ on the metamagnetic transition in TbAlG gives a basis for assuming an analogy[30] between the induced moment at 0 °K in TbAlG and the Kramers doublet at $T \neq 0$ °K in the case of DyAlG.

An interesting situation occurs in HoAlG, for which the condition $\Delta/2\gamma m_s^2 = 1.009$ is realized. The values of T_N of the garnet, as also of the terbium and holium gallates, which have the lowest T_N's, can be explained only with allowance for the energy of hyperfine interaction. To describe the properties of these compounds, Hammann and Manneville[24,25] used a Hamiltonian of the form

$$\mathcal{H} = \mathcal{H}_c - g_J\mu_B JH - a_J JI;$$

here $\mathcal{H}_c$ is the two-singlet crystal-field Hamiltonian, while the last term takes account of the magnetic-dipole part of the hyperfine interaction (it is assumed that the electric-quadrupole part is considerably smaller); a_J is the hyperfine-interaction constant, and I is the nuclear spin. In the molecular-field approximation, an expression was found for T_N, which depends on $a_J^2(I+1)$ as well as on the values of Δ and γ. By using the values of Δ given in Table II and values of γ calculated in the dipole–dipole interaction approximation, the authors of[24] obtained $T_N^{theor} = 0.34$ °K for TbGaG and $T_N^{theor} = 0.103$ °K for HoGaG. These values are in satisfactory agreement with the experimental T_N's (see Table II) obtained from measurements of heat capacity and susceptibility.

Information about the magnitudes of exchange interactions in rare-earth gallates was obtained by Onn and co-workers,[16] who made measurements of the heat capacity of Nd, Sm, Gd, Er, Dy, Ho, and Yb gallates in the range 0.35–4 °K. Detailed study of antiferromagnetic ordering of neodymium, samarium, and erbium gallates has established that the properties of these garnets are described by a Heisenberg model of an antiferromagnet with $s = \frac{1}{2}$. On assumption of a Hamiltonian of the form

$$\mathcal{H} = -2J_{cc}s_1s_2$$

values were obtained for the R^{3+}–R^{3+} exchange-interaction integrals. An estimate of the contribution of dipole–dipole interaction to the heat capacity showed that it amounts to about 30% in the case of erbium gallate and

TABLE III. Exchange-interaction integrals obtained from calorimetric data.[16]

Garnet	$C_{mag}T^2/2R$	J, °K	E/R	J, °K	T_N, °K	J, °K
NdGaG	0.16	0.32	0.47	0.36	0.516	0.38
SmGaG	0.60	0.63	0.87	0.67	0.918	0.68
ErGaG	0.43	0.53	0.73	0.56	0.789	0.58

is negligibly small for samarium and neodymium gallates. For comparison we note that in DyAlG the dipole–dipole interactions give a contribution of about 70%.[32]

The exchange-interaction parameters J_{cc} obtained from the high-temperature "tail" of the specific heat, from the magnetic energy, and from T_N (the high-temperature expansion), according to the data of[16], are shown in Table III. (Here and hereafter we shall denote by J_t the value of J_t/k in °K.)

All three methods of determining J_{cc}, which agree quite well with one another, assume that the magnetic ordering is caused entirely by exchange interaction. This is obviously fulfilled well for the Nd and Sm gallates and to a lesser degree by erbium gallate.

B. Magnetic phase diagrams. Pecularities of the properties of DyAlG near the tricritical point

Investigation of the magnetic properties of HoAlG at extremely low temperatures[23] has established that in this compound, below the magnetic ordering temperature, the nature of the phase transition depends on the direction of the external field with respect to the crystallographic axes of the crystal. This is evidenced by the results of measurements of the differential susceptibility of HoAlG at 0.36 °K (Fig. 5). As is seen from Fig. 5a, the dependence of dM/dH on H along a [111] axis reveals considerable hysteresis. The mildly sloping part of the maximum of dM/dH is characteristic of the disappearance of the metastable phase (antiferromagnetic on increase of field, paramagnetic on decrease). On the same crystal along a [001] axis, an ordinary phase transition of the second kind is observed (Fig. 5b). The phase diagram of HoAlG obtained experimentally at 0.36 °K (Fig. 6) agrees well with theoretical calculations for the two-singlet model in the molecular-field approximation.[30]

The phase diagram of TbAlG, constructed according

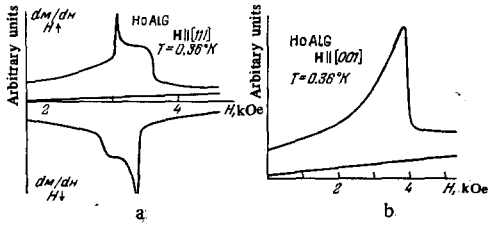

FIG. 5. Variation of dM/dH of HoAlG at 0.36 °K with external magnetic field H, applied along axes: (a), [111]; (b), [001].

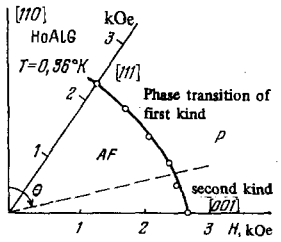

FIG. 6. Magnetic phase diagram of a HoAlG monocrystal ($T = 0.36$ °K).

to magnetic data,[22] is given in Fig. 7. In this garnet, for $H_0 \parallel [111]$, the line of phase transitions of the first kind above a certain temperature T_{cr} changes to a line of phase transitions of the second kind.

Precision magnetic and calorimetric investigations of a monocrystal of DyAlG[33] have made it possible to construct, for this garnet, the phase diagram shown in Fig. 8. Characteristic of the phase diagram of DyAlG, when the external field $H_0 \parallel [111]$, is the existence of a tricritical point with the coordinates $T_t = 1.66$ °K, $M_t = 250$ cgs emu/cm^3, $H_t^{\pm} = 3.25$ kOe. For temperatures below 1.66 °K, phase transitions of the first kind are observed in a DyAlG specimen. But the interpretation of the experimental results here is complicated because of rather large demagnetizing effects, since in a crystal of finite dimensions the demagnetizing field "smears" the transition over a field interval

$$H_0^- < H_0 < H_0^+,$$

where

$$H_0^+ = H_0^- + N(M^+ - M^-).$$

If one makes a correction for the demagnetizing field ($N = 0$), then one obtains for DyAlG the line of phase transitions shown dotted in Fig. 8. There is interest in the experimental study of DyAlG in the immediate vicinity of T_t, because a number of theoretical papers[34–36] have predicted the asymptotic behavior of various systems, including magnetic systems, near tricritical points. But difficulties connected with allowance for the demagnetizing fields and with determination of the beginning of a phase transition of the first kind prevented for a quite long time the obtaining of unambiguous results for DyAlG.[37,38] Only recently have Wolf and Giordano[39] succeeded, by a new method based on study of the dynamic magnetization of DyAlG near T_t, in finding the values of the four critical exponents β_u, γ_u, δ_+, and δ_-; here β, γ, and δ are the critical exponents for, respectively, the magnetization $M(T, H=0)$, the susceptibility, and the critical isotherm. For the range

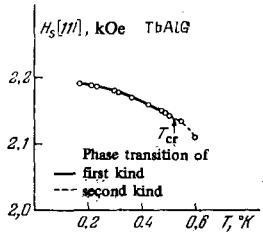

FIG. 7. Magnetic phase diagram of TbAlB along [111] axis.

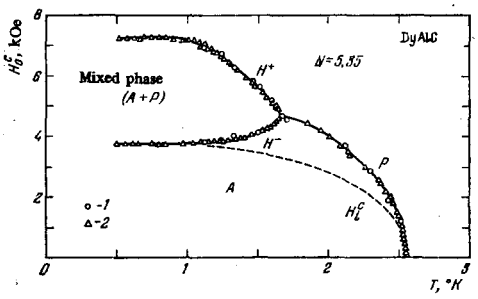

FIG. 8. Magnetic phase diagram of DyAlG according to data from: (1) measurements of the magnetic moment; (2) measurements of the specific heat. Dotted line: experimental data converted to $N = 0$.

$0.1 > \varepsilon \equiv (T - T_t)/T_t > 0.003$, the values obtained agree well with scaling predictions for the tricritical point ($\beta_u = \gamma_u = 1$, $\delta = 2$).

Additional information about features of the phase transition in DyAlG has been obtained by Dillon and coworkers,[40,41] who investigated the magneto-optical properties near the tricritical point. The most interesting result of these researches consists in the observation of two essentially different antiferromagnetic states (A^+ and A^-), depending on the magnetic prehistory of the specimen. Also established was the existence of hysteretic effects in the magnetic field range that describes the beginning of the metamagnetic transition (at $T = 1.27$ °K).

By means of a polarizing microscope, the authors[41] succeeded in tracing the dynamics of the appearance and coexistence of three phases: two antiferromagnetic (A^+ and A^-) and a paramagnetic (P^+). This is illustrated by Fig. 9, which shows microphotographs obtained on a DyAlG

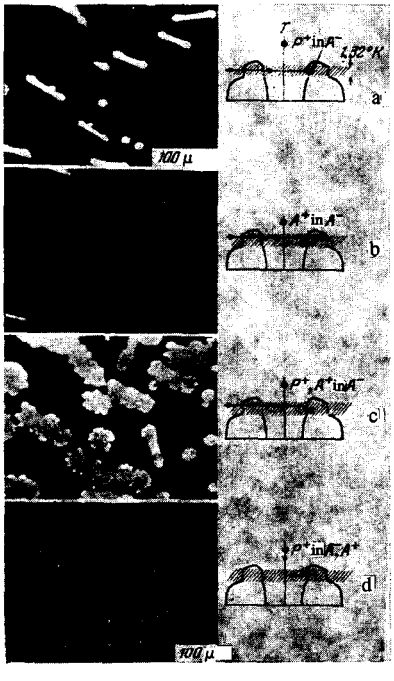

FIG. 9. Microphotographs of magnetic phases A^+, A^-, and P^+ in thin plates of DyAlG (a–c, 690 μm; d, 190 μm), at various fields and temperatures. The right part of the figure shows the scheme for reaching the prescribed T and H.

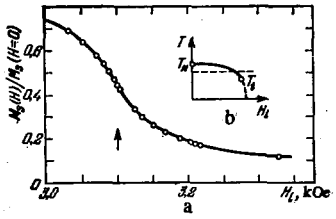

FIG. 10. Field dependence of sublattice magnetization of DyAlG at $T = 1.885$ °K (a). The change of field corresponds to the dotted line on the phase diagram (b); the arrow shows the field corresponding to crossing of the phase boundary.

crystal at 1.32 °K. The right part of the figure shows schematically the change of the magnetic field applied to the specimen, whose original phase was A^-. In Fig. 9a, the field has just transformed the specimen to a mixed phase: light nuclei of P^+ are visible against a dark background of phase A^-. If the field is now diminished to a value where only phase A^+ is stable, the P^+ regions will be transformed to A^+; and this is illustrated in Fig. 9b, where A^+ is visible in A^-. The contrast here is not too great, since the difference of magnetizations is much smaller than in the case of phases A^- and P^+. When the field is again increased, nucleation of P^+ occurs once more; and now all three phases are observed simultaneously (Fig. 9c). The phase P^+ is nucleated on the A^+–A^- boundary, "decorating," as it were, the antiferromagnetic domain walls. Figure 9d shows the results of an experiment in which there occurred cooling from $T > T_N$, in zero magnetic field, and at 1.32 °K a transition of the specimen to the mixed-phase region. Here a multitude of fine "needles" of the paramagnetic phase P^+ appear against a background of A^+ and A^-.

An explanation of the characteristics of the magnetic phase transiton in DyAlG was given by Blume and coworkers[42,43] and by Wolf.[44] They showed that the symmetry of DyAlG allows an interaction between the antiferromagnetic order parameter

$$\eta = M_b - M_a$$

(a and b are two types of nonequivalent Dy^{3+} sites in the dodecahedral sublattice) and the applied field, so that in fact there is no temperature at which $\eta = 0$ in the presence of a field. This has been corroborated by experiments[42] on scattering of neutrons by DyAlG in an external magnetic field parallel to a [111] axis. It was shown that Bragg elastic scattering does not vanish at the phase boundary but has only an inflection point, with a long tail in the paramagnetic region (Fig. 10); that is, long-range antiferromagnetic ordering persists in the region that has been considered paramagnetic.

Such interactions have been well studied in antiferromagnets with weak ferromagnetism,[4,5] for which the free energy contains a term proportional to ηH. But in DyAlG the occurrence of a spontaneous moment is not allowed by the crystal symmetry, and the corresponding term is written in the form $\eta H_x H_y H_z$, which is equivalent to an induced field H_s nonuniform through the specimen (staggered magnetic field); and this leads to a term ηH_s in the free energy. According to the data of[44], for external field 3 kOe and $T = 1.3$ °K, $H_s \approx 1$ Oe;

but this proves sufficient for the occurrence of two metastable states (A^+ and A^-) and for a change of character of the phase transition near T_t.

Since for the two other principal axes of DyAlG, [001] and [110], there is no interaction between the order parameter and the external field ($H_x H_y H_z = 0$), here ordinary phase transitions of the second kind should be observed. For these directions there are so far rather few experimental data.[27,45] Wolf,[44] however, suggests the existence of low-temperature phase transitions of the second kind ($T \approx 1$ °K for $H_0 \parallel [001]$ and $T \approx 0.6$ °K for $H_0 \parallel [110]$) in sufficiently strong magnetic fields $H > 5$ kOe, which the author relates to ordering of spins that are perpendicular to the applied field and consequently do not interact with it. A discussion of these unusual phase transitions is given in[27,31,45].

C. Ordering of Fe^{2+} and Mn^{2+} ions in dodecahedra

Antiferromagnetic ordering in garnets containing 3*d* ions in the dodecahedral sublattice was discovered by Prandl[46] through data on neutron diffraction and magnetic susceptibility. It was established that almandite, $Fe_3Al_2Si_3O_{12}$, has $T_N = 7.5$ °K, and that its cubic elementary cell coincides with the magnetic cell in the antiferromagnetic phase. Further investigations of mono- and polycrystalline speciments of this garnet were made by Mössbauer spectroscopy.[47,48] The best agreement of the experimental Mössbauer spectra with the theoretical is achieved by assuming that the antiferromagnetism vector in almandite lies along a [100] axis. This made it possible to find the temperature dependence of the effective magnetic field acting on the nuclei of the Fe^{2+} ions and to determine the Néel point: $T_N = 5.5 \pm 0.1$ °K. The considerable difference from the T_N obtained in[46] is attributed by the authors of[47] to a different content of Fe^{2+} ions in the almandite crystals (the limiting FeO content is about 43 wt. %); and the rather low value of H_{eff} at $T = 0$ °K (250 kOe) is explained, according to[47], by a large positive contribution to this field from the incompletely quenched orbital moment of the Fe^{2+} ions.

Antiferromagnetic ordering of Mn^{2+} ions on dodecahedral sites of garnets was established simultaneously by Prandl[49] and by Plumier[50] by experiments on neutron diffraction of the garnet $Mn_3Al_2Ge_3O_{12}$ (MnAlG) at 4.2 °K. This garnet is essentially the only antiferromagnetic garnet in which all the *c* sites are occupied by magnetic *s* ions (Mn^{2+}) (cadolinium gallate does not become ordered down to 0.3 °K[151]). To describe the antiferromagnetic ordering in MnAlG, the authors of[49,50] suggested three magnetic structures, only one of which agrees with those predicted by Capel.[26] But an analysis of exchange bonds of Mn^{2+} in the dodecahedral sublattice of the garnet, carried out in[51], enables us to make a choice in favor of Prandl's model, which is not predicted by theory. In this structure (Fig. 11), the magnetic moments of all the Mn^{2+} atoms lie in a (111) plane and are directed along or opposite to one of the three crystal axes $[2\bar{1}\bar{1}]$, $[\bar{1}2\bar{1}]$, $[\bar{1}\bar{1}2]$.

Measurements of the heat capacity of MnAlG[51] have established that for this garnet $T_N = 6.65 \pm 0.05$ °K, and the value of the total change of entropy agrees well with the theoretical value for $s = \frac{5}{2}$. Above T_N, the temperature dependence of the inverse susceptibility of MnAlG follows the Curie–Weiss law with effective magnetic moment 5.89 μ_B, close to the value $g\sqrt{s(s+1)} = 5.92\ \mu_B$ for $g = 2$ and $s = \frac{5}{2}$. Measurements in pulsed magnetic fields made possible a determination of the spin-flip ("collapse") field in MnAlG: $H_E(3\ °K) = 210$ kOe.[51]

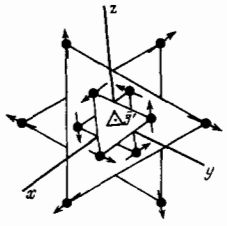

FIG. 11. Magnetic structure of MnAlG (projection on (111) plane).

In contrast to the octahedral and tetrahedral site of the garnet, in which the magnetic atoms are coupled by exchange chains consisting, as a minimum, of two oxygen atoms, nearest neighbors in dodecahedral positions are coupled by indirect exchange interaction in which a single intermediate oxygen atom takes part. Bonds with the second, third, etc. coordination spheres occur by chains consisting of at least two oxygen atoms. But in these cases it is difficult to select any predominant chain, because, in consequence of the high coordination of the oxygen polyhedron ($z = 8$), several approximately equivalent bonds of different type are formed at once between the magnetic atoms, and this leads to some averaging of the values of the exchange parameters. With allowance for this situation, the following values were obtained[51] for the exchange-interaction integrals of MnAlG: $J_1 = -0.57$ °K, $\bar{J}_2 = -0.12$ °K. Here $\bar{J}_2$ represents a certain average value for interactions that involve participation by no fewer than two intermediate links ($\bar{z}_2 = 22$).

3. GARNETS WITH MAGNETIC IONS IN OCTAHEDRA

Garnets have now been synthesized that contain practically all the 3*d* ions, and also ions of the heavy rare earths (Dy–Yb), in the *a* sublattice.[52–54] Such broad "opportunities" for octahedral sites are due to the fact that the oxygen octahedra in the garnet structure are not geometrically accurate: they are distorted in some degree. Thus ions with an arbitrary electronic configuration can go into octahedral sites of a garnet if their dimensions permit it. The ions Fe^{3+} and Co^{2+}, as was shown by the investigations[55,56], occupy only *a* positions. The choice of nonmagnetic ions to enter the *c* and *d* sublattices is dictated by the crystal chemistry of the garnet: in the case of trivalent 3*d* ions, $Ca_3Me_2^{3+}Ge_3O_{12}$ (MeGeG); for bivalent 3*d* ions, $NaCa_2Me_2^{2+}V_3O_{12}$ (MeVG); in the synthesis of garnets with rare-earth ions in octahedra, the *c* sites are blocked by the large Ca^{2+} or Sr^{2+} ions.

Experimental demonstration of antiferromagnetic ordering in the *a* sublattice was first accomplished by Bozorth and Geller[11] in an investigation of the mag-

netic susceptibility of the garnet $Ca_2Fe_2Ge_3O_{12}$. A synthesis and investigation of polycrystalline garnets containing the ions Cr^{3+}, Mn^{3+}, Co^{2+}, Ni^{2+}, and Cu^{2+} in octahedra was described in[57]; later, monocrystalline specimens of some of these garnets[58] were also studied, and antiferromagnetic ordering was discovered in the garnet with Mn^{2+}.[59] Table IV gives the lattice parameters and basic magnetic characteristics of garnets with 3*d* ions in octahedra. Here all the notation is the same as in Table I, and H_E is the "collapse" field of the antiferromagnet.

A. Magnetic structures. Exchange-interaction integrals

Neutron-diffraction investigations[59-64] at 4.2 °K have shown that, depending on the 3*d* ion in the octahedral sublattice of the garnet, three types of magnetic structures are observed below T_N (Fig. 12). The simplest and also the most widespread for antiferromagnetic garnets with 3*d* ions is the magnetic structure shown in Fig. 12c: two cubic ferromagnetic sublattices, one inserted antiferromagnetically into the other (ordering of the first kind according to Smart[65]). This structure, according to neutron-diffraction data, occurs in CrGeG, MnVG, CoVG, and NiVG.

Figure 12a shows the magnetic structure found by Plumier[60] and by Prandl[64] for FeGeG. As is seen from the figure, it is a set of two cubic lattices, each of which is ordered antiferromagnetically. The direction of the spins in these sublattices is collinear (antiferromagnetic ordering of the second kind). But there is an indication that for FeGeG there may occur the same structure but with a noncollinear spin arrangement.[66]

The magnetic configuration of MnGeG (Fig. 12b), according to Plumier,[63] is formed by ferromagnetic chains along one of the cube edges [001]; the direction of the spins reverses on translation along the [100] and [010] axes. This is antiferromagnetic ordering of the third kind, which according to molecular-field theory[65] occurs only when there is tetragonal distortion of the cubic lattice. Apparently such distortion in a garnet with Mn^{3+} in octahedra can be produced by the Jahn-Teller effect (see note 1 added in proof, p. 164).

Application of the molecular-field method to the space-centered cubic lattice of a garnet enables us to find the relation between the experimental values of C, Θ_p, and T_N (see Table IV) and the molecular-field coefficients for nearest (γ_1) and next-nearest (γ_2) neighbors. According to[65] we have in the case of antiferromagnetic ordering of the first kind

$$T_N = -C(\gamma_1 - \gamma_2), \quad \Theta_p = C(\gamma_1 + \gamma_2). \tag{5}$$

For ordering of the second kind

$$T_N = -C\gamma_2, \quad \Theta_p = C(\gamma_1 + \gamma_2). \tag{6}$$

By using the relation

$$\gamma_{1,2} = \frac{2z_{1,2}J_{1,2}}{2Ng^2\mu_B^2} \tag{7}$$

(z is the number of neighbors, N Avogadro's number) and experimental values of the g factor,[67] one can determine the exchange integrals J_1 and J_2. Table V shows J_1 and J_2 found by this method for garnets with octahedral ions Cr^{3+}, Mn^{2+}, Fe^{3+}, and Co^{2+}. Because, as will be shown below, in the case of NiVG at $T < T_N$ equation (5) is inapplicable, in order to estimate the Ni^{2+}–Ni^{2+} exchange interactions use was made of the experimental value[1)] of H_E and of data from calorimetric measurements.[67] As is seen from Table V, the exchange interactions in CoVG are considerably stronger than the cooresponding interactions Cr^{3+}–Cr^{3+}, Ni^{2+}–Ni^{2+}, and Fe^{3+}–Fe^{3+} in the octahedral sublattice of a garnet. It is possible that the reason for this difference lies in the fact that J_1 and J_2 in CoVG are effective values containing an appreciable contribution from anisotropic exchange interaction (see note 2 added in proof, p. 165).

The peculiarities of the magnetic structure of MnGeG lead to the result that a determining role in the Mn^{3+}–Mn^{3+} exchange interaction is played by six nonequivalent (because of the tetragonal distortion of the lattice) next-nearest neighbors. Molecular-field theory gives the following relation for antiferromagnetic ordering of the third kind:

$$T_N = \frac{2}{3}s(s+1)(-4J_2+2J_3), \quad \Theta_p = \frac{2}{3}s(s+1)(8J_1+4J_2+2J_3). \tag{8}$$

To determine the exchange integrals, one may obviously use as a third equation the expression for the specific heat above T_N given by the high-temperature expansion method.[68]

TABLE IV. Lattice parameters (a_0), Néel temperatures (T_N), constants in the Curie-Weiss law (Θ_p and C_m), and collapse field (H_E) of garnets with octahedral 3*d* ions.

Garnet	$a_0 \pm 0.002$ Å	T_N, °K	Θ_p, °K	C_m, cgs emu/mol	H_E, kOe (4.2 °K)
CrGeG	12.260	12.6	−21.4	3.91	256
MnVG	12.565	25.5	−48.5	8.8	—
MnGeG	12.315	13.85	−14.5	6.84	—
FeGeG	12.322	12.2	−65	10	404
CoVG	12.451	6.40	−17.5	4.76	120
NiVG	12.371	7.9	−11.0	2	294
CuVG	12.427	—	−3.0	0.57	—

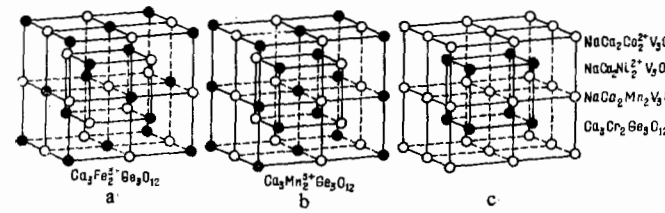

FIG. 12. Magnetic structures of garnets containing 3*d* ions (in *c*, ions Mn_2^{2+}, Cr_2^{3+}) in octahedra.

[1)] In the molecular-field approximation, it is easy to show that for magnetic ordering of the first kind $H_E(T) = -2\gamma_1 M_s(T)$.

TABLE V. Exchange integrals of garnets with 3*d* ions in octahedra.

3*d* ion in garnet	Cr^{3+}	Mn^{2+}	Co^{2+}	Ni^{2+}	Fe^{3+}	Mn^{3+}
J_1, °K	−0.81	−0.80	−2.94	−1.27	−0.80	−1.33
J_2, °K	−0.28	−0.32	−1.81	−0.60	−0.36	+0.45 ($J_3 = +2.63$)

$$\frac{C_M T^2}{R} = \frac{1}{3} s^2 (8s+1)^2 (J_1^2 + 4J_2^2 + 2J_3^2). \quad (9)$$

The values of J_1, J_2, and J_3 obtained by means of equations (8) and (9) for Mn^{3+} (see Table V) show that in the MnGeG lattice, the ferromagnetic interaction within chains (J_3) proves to be the interaction of actually nearest neighbors (the strongest). The weakest is that between chains (J_2). Such a relation of exchange interactions is characteristic of metamagnets. In fact, a metamagnetic transition has been observed[57] in MnGeG; it will be considered in detail below.

The mechanism of the negative exchange interaction that causes the antiferromagnetism of garnets with 3*d* ions in the octahedra has so far received very little investigation. There are only indications[60,69] that for Fe^{3+} the indirect exchange interaction is produced either through two oxygen ions ($Fe^{3+}-O^{2-}-O^{2-}-Fe^{3+}$) that form a common edge of a tetrahedron and a dodecahedron, or through the same oxygen ions and a tetrahedral cation located between them ($Fe^{3+}-O^{2-}-Ge^{4+}-O^{2-}-Fe^{3+}$). In the case of CoVG and NiVG, study of NMR in V[51] has shown that the vanadium ion does not take part in the exchange.[70]

In closing our discussion of exchange interactions in garnets with octahedral 3*d* ions, we must mention that for FeGeG, molecular-field theory predicts antiferromagnetic ordering of the first kind (on the basis of the ratios $\theta_p/T_N = 5.3$ and $\gamma_2/\gamma_1 = 0.33$), whereas experiment (research on neutron diffraction in FeGeG has been conducted independently in three laboratories[60,62,64]) gives ordering of the second kind. The reason for this is not yet clear.

B. 3*d* ions in the octahedral crystalline field of a garnet

For garnets containing 3*d* ions, as for many compounds of elements of the iron group, the relation $E_{cr} \gg E_{LS}$ is valid; that is, the electrostatic crystalline field is large enough to decouple the angular momenta L and S. This effect causes "quenching" of the orbital angular momentum and enables us to use, for description of the properties of garnets with 3*d* ions in octahedra, the spin-Hamiltonian method developed by Abragam and Pryce.[71]

The nature of the splitting of the energy levels of the 3*d* electrons under the action of the crystalline field is determined to a considerable degree by the symmetry of the problem. The environment of a magnetic ion in octahedra of a garnet is not strictly cubic: as a rule, there is a slight trigonal distortion of the octahedron along a space diagonal of the cube.[72] Since the cubic part of the crystalline potential considerably exceeds in magnitude the components of lower symmetry, the splitting of the terms of the free 3*d* ions is determined, in first approximation, by the cubic field and occurs in such a way that the ground state for octahedral ions $Cr^{3+}(d^3)$, $Mn^{3+}(9d^4)$, Mn^{2+}, $Fe^{3+}(d^5)$, $Co^{2+}(d^7)$, and $Ni^{2+}(d^8)$ will be, respectively, Γ_2, Γ_3, Γ_1, Γ_4, and Γ_2.

We shall consider, for the example of d^5, d^7, and d^8 ions, how the further lifting of the degeneracy proceeds.

1. *Ground state an orbital singlet* (Ni^{2+}, Cr^{3+}). Without allowance for hyperfine interaction, the spin Hamiltonian has the form

$$\hat{\mathcal{H}} = \mu_B g_{ij} H_i \hat{S}_j + D_{ij} \hat{S}_i \hat{S}_j. \quad (10)$$

The first term describes the splitting of the levels in the external magnetic field. The second term describes the splitting of the ground state in the noncubic crystalline field. With trigonal distortion of the octahedron along the z axis, (10) takes the form

$$\mathcal{H} = \mu_B [g_{\parallel} H_z s_z + g_{\perp} (H_x s_x + H_y s_y)] + D\left[s_z^2 - \frac{1}{3} s(s+1)\right]. \quad (11)$$

For NiVG below T_N, in the absence of an external field, we have

$$\mathcal{H} = g\mu_B H_{\text{eff}}\, s + D\left[s_z^2 - \frac{1}{3} s(s+1)\right], \quad (12)$$

where H_{eff} is the effective molecular field exerted on the Ni^{2+} by the magnetic atoms surrounding it. In the Heisenberg exchange-interaction approximation,

$$g\mu_B H_{\text{eff}}\, s_i = 2 \sum_{i \neq j} J_{ij} s_i s_j. \quad (13)$$

The coefficient D is (12) characterizes the splitting of the levels in the trigonal field.

According to measurements of the optical absorption spectra made on NiVG at 4.2 °K, $D = 6.79$ cm^{-1}.[73] A schematic of the splitting of the energy levels and $10Dq$ of Ni^{2+} on octahedral sites of a garnet, at helium temperatures, is given in Fig. 13. We note that the value of the splitting of the ground energy level of Ni^{2+} in the trigonal crystalline field of the garnet ($D/k \approx 8.7$ °K) is comparable with the splitting by the exchange field at 0 °K ($T_N = 7.9$ °K). This fact leads to two important consequences. First, the levels in the exchange field are significantly nonequidistant; therefore equation (5) ceases to be satisfied for the nickel garnet. And sec-

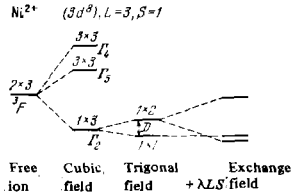

FIG. 13. Energy levels of Ni^{2+} on octahedral sites of a garnet, at $T < T_N$.

ond, for $T \gg T_N$, when the splitting by the exchange field is small, there should be observed a contribution to the specific heat of the Schottky type, caused by transitions between levels with splitting D/k.

2. *Ions in an s state* (Fe^{3+}, Mn^{2+}). EPR investigations on octahedral ions Fe^{3+} [72] and Mn^{2+} [74] in a YGaG matrix have shown that for analysis of the spectra of these ions, the following Hamiltonian may be used:

$$\mathcal{H} = g\mu_B Hs + D[s_\xi^2 - 1/3s(s+1)] + \frac{1}{6}a[s_x^4 + s_y^4 + s_z^4 - \frac{1}{5}s(s+1)(3s^2+3s-1)] + \frac{1}{180}F[35s_\xi^2 - 30s(s+1)s_\xi^2 + 25s_\xi^2 - 6s(s+1) + 3s^2(s+1)^2]. \quad (14)$$

with effective spin $s = \frac{5}{2}$. Here D and F are terms of the second and fourth order, describing an axial field, with axis ξ lying along the trigonal axis of the crystal; a is the splitting parameter of the cubic crystalline field with axes x, y, and z (axes of fourth order), no one of which in general coincides with the axis ξ. In zero magnetic field H and in the absence of exchange interaction, the lowest levels of Fe^{3+} represent three Kramers doublets, the distances between which are small. For $CaSc_2Ge_3O_{12}$ garnet with small additions of Fe^{3+} in octahedra, [75] $D = -0.0375$ cm^{-1} and $a - F = 0.0096$ cm^{-1}. It should be mentioned that in the same paper a correlation was found between the value of D and the trigonal distortion of the octahedron; on this basis it was deduced that covalence makes a large contribution to the value of D.

Figure 14 shows the schematic of the energy levels of Fe^{3+} (and Mn^{3+}) (at 4.2 °K) with allowance for the effective exchange field.

3. *Triplet orbital ground state* (Co^{2+}). According to detailed EPR investigations of Co^{2+} in a YGaG monocrystal at 4.2 °K, [76] the octahedral cobalt ion is described by the level-splitting schematic shown in Fig. 15.

In the field of trigonal symmetry, the triplet Γ_4 splits into a lower doublet and an upper singlet. Spin-orbit coupling leads to a further lifting of the degeneracy and to the formation of six Kramers doublets. It is obvious that splitting of this state can occur only under the influence of an external or of an exchange field (the magnetic-moment operator in the Hamiltonian changes sign under time reversal). The fundamental parameters that describe the interaction of the Co^{2+} ion with the octahedral crystalline field of the garnet are[76]: the splitting by the cubic field $10Dq = 800$ cm^{-1}, the trigonal field parameter $\Delta_t = 650$ cm^{-1}, and the spin-orbit splitting $\alpha\lambda \approx 200$ cm^{-1}.

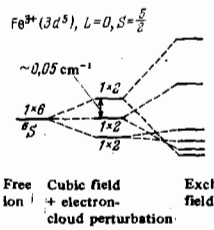

FIG. 14. Energy level of Fe^{3+} on octahedral sites of a garnet, at $T < T_N$.

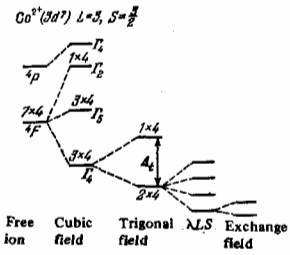

FIG. 15. Energy levels of CO^{2+} on octahedral sites of a garnet, at $T < T_N$.

At helium temperatures, only the lowest Kramers doublet is occupied; therefore the behavior of octahedral Co^{2+} ions in the garnet is described by the spin Hamiltonian, with effective spin $s = \frac{1}{2}$,

$$\mathcal{H} = g_{\parallel}\mu_B H_z s_z + g_{\perp}\mu_B(H_x s_x + H_y s_y) + AS_z I_z + B(S_x I_x + S_y I_y), \quad (15)$$

where $g_{\parallel} = 7.027$, $g_{\perp} = 2.665$, $|A| = 307.5 \cdot 10^{-4}$ cm^{-1}, $|B| = 15 \cdot 10^{-4}$ cm^{-1}, $I = \frac{7}{2}$. The appreciable difference from the g factor of the free Co^{2+} ion is explained[76] by the effect of admixture to the Γ_4 level from the upper excited states, $-{}^4P$, and also Γ_5 and Γ_2.

It should be mentioned that the results of investigation of the optical spectra of CoVG at 4.2 °K[73] differ somewhat from the energy-level scheme discussed above for the Co^{2+} ion in a diamagnetic matrix of YGaG. The magnitude of the trigonal splitting is appreciably larger, $\Delta_t = 1050$ cm^{-1}; furthermore, it is noticed that the ground level in the cubic field Γ_4 (see Fig. 15) splits in a field of lower symmetry in such a way that it is the orbital singlet that is lower, and not the doublet, as follows from the EPR data on Co^{2+}. The reason for this discrepancy is not completely clear. It can only be hypothesized that the presence in $NaCa_2Co_2V_3O_{12}$ of the ions of different valences Na^+ and Ca^{2+} distorts the oxygen octahedron, and that the symmetry becomes lower than trigonal (the idea is due to M. D. Sturge, private communication). This assumption is in harmony with data of [77] on EPR study of V^{4+} in the garnet $NaCa_2Mg_2V_3O_{12}$: an anomalous broadening of the EPR line was found, which is associated with Na^+ and Ca^{2+} ions in dodecahedra.

C. Specific heat. Behavior in a strong magnetic field

For the purpose of obtaining information about the characteristics of the paramagnetism–ferromagnetism phase transition, the specific heat was investigated in garnets containing 3d ions in octahedra. [67,78-83] For illustration, Figs. 16 and 17 show the results of measurements of the specific heat for FeGeG and CoVG. Also shown there is the magnetic entropy, calculated by integration of the experimental C_{mag}/T curves in the interval 2–26 °K. In order to obtain the total change of entropy $\Delta S|_0^\infty \equiv S_\infty - S_0$, an extrapolation was made: in the temperature range 0–2 °K according to the law $C \propto T^3$, and for $T > 26$ °K according to the law $C \propto aT^{-2}$. Since for $T > T_N$ the specific heat of antiferromagnetic garnets varies as

$$C = aT^{-2} + bT^3, \quad (16)$$

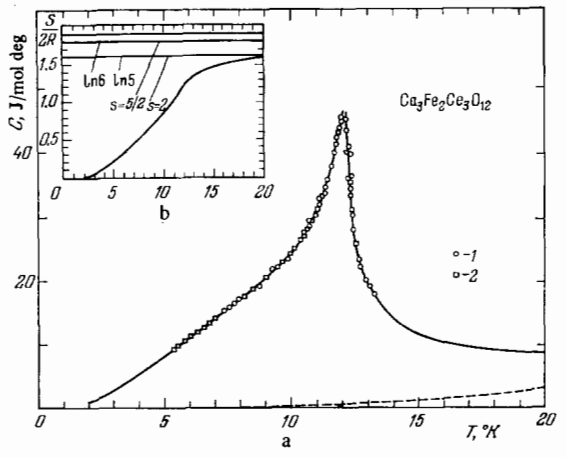

FIG. 16. a) Temperature dependence of specific heat of FeGeG in zero magnetic field (solid line) and at $H \neq 0$. b) Temperature dependence of entropy. Points: 1, $H = 30$ kOe; 2, $H = 45$ kOe. Dotted line, lattice specific heat.

the variation of CT^2 with T^5 makes it possible to find the the lattice contribution to the specific heat and to determine the Debye temperature (Θ_D). The values of Θ_D and also the critical values of the entropy and the internal energy (E) are given in Table VI. The calculation of the internal energy was made on the basis of the specific-heat data ($E = \int_0^T C_{mag}\,dT$), with extrapolation according to the same laws as for the entropy.

The contribution of the nuclear specific heat in the helium-temperature range has been established experimentally only for MnGeG.[67] For other garnets with $3d$ ions, its value does not exceed (according to estimates) 0.2% of the total specific heat of the specimens. For comparison with experiment, Table VI gives theoretical values of the entropy and internal energy obtained for the Heisenberg and Ising models.[84-86] It is seem that the experimental values of ΔS and ΔE are closer to the Heisenberg model of an antiferromagnet, a characteristic of which is the existence of a long "tail" of the specific heat (short-range order for $T > T_N$), and therefore the ratio $(E_N - E_\infty)/(E_0 - E_N)$ is appreciably larger than 1.

Since the change of entropy upon transition of the system to the ordered state is $R\ln(2s+1)$, the experimental value of $\Delta S|_0^\infty$ enables us to obtain information about the multiplicity of the ground state of the octahedral $3d$ ions.

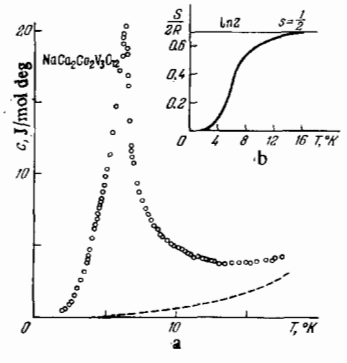

FIG. 17. a) Specific heat of CoVG at $H = 0$ (circles) and lattice contribution (dotted line). b) Temperature dependence of entropy for cobalt garnet.

TABLE VI. Critical values of entropy (S) and internal energy (E) for garnets with $3d$ ions in octahedra. (s_{eff} is the effective spin of the ion, calculated from the value of $\Delta S|_0^\infty$).

Garnet	s_{eff}	$\frac{\Delta S}{2R}\Big\|_0^\infty$	$\frac{\Delta E}{2R}\Big\|_0^\infty$	$\frac{S_\infty - S_N}{2R}$	$\frac{S_N - S_0}{2R}$	$\frac{E_N - E_\infty}{2RT_N}$	$\frac{E_0 - E_N}{2RT_N}$	$\frac{E_N - E_\infty}{E_0 - E_N}$
CoVG	0.55	0.74	0.98	0.34	0.40	0.68	0.30	2.22
NiVG	1	1.0	1.40	0.45	0.65	0.95	0.45	2.11
CrGeG	1.75	1.52	1.56	0.45	1.07	0.84	0.72	1.16
MnGeG	2	1.63	1.69	0.51	1.12	0.945	0.745	1.23
FeGeG	2.3	1.72	1.76	0.52	1.20	0.97	0.79	1.22
Heisenberg model (bcc)	1/2	0.693	0.757	0.235	0.458	0.460	0.297	1.55
Ising model (bcc)	1/2	0.693	0.629	0.107	0.586	0.169	0.460	0.37

For NiVG and MnGeG the value of the total change of magnetic entropy agrees well with the theory for $s = 1$ and $s = 2$, respectively (see Table VI). This indicates that in the process of ordering of the garnets, all three components of the ground state of Ni^{2+} are occupied, and five components of the ground state of Mn^{3+}.

In the case of CoVG, the specific-heat measurements substantiate that the ground state of the Co^{2+} at helium temperatures is a Kramers doublet. As is seen from Fig. 17b, the entropy of CoVG has already reached the theoretical value for $s = \frac{1}{2}$ at 16 °K; that is, at this temperature the lower doublet is fully populated, and with rise of temperature population of the higher-lying doublet proceeds. Therefore, obviously, at $T > T_N$ the specific heat contains a contribution due to transitions to the higher-lying levels, and this produces an exaggerated "tail."

For FeGeG, the experimental values of $\Delta S|_0^\infty$ is close to the expected value for Fe^{3+} spin $s = \frac{5}{2}$, but not all six levels are occupied during the process of antiferromagnetic ordering: at 20 °K the entropy approaches only the value corresponding to $s = 2$ (Fig. 16b).

Measurements of the specific heat of FeGeG in magnetic fields of 30 and 45 kOe (Fig. 16a) revealed no difference from the function $C(T)$ at $H = 0$.[78] A different situation is observed for CoVG (Fig. 18): although the

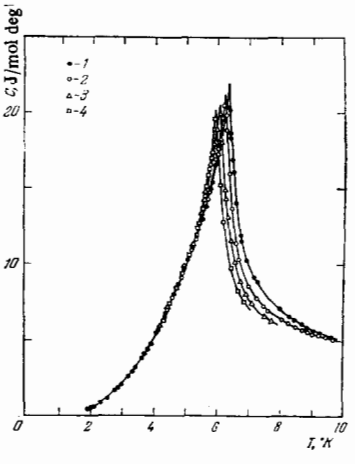

FIG. 18. Specific heat of CoVG in an external magnetic field. H (kOe); 0.5; 10; 20 (1), 30 (2), 40 (3), and 45 (4).

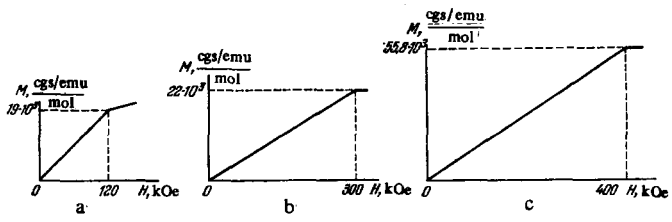

FIG. 19. Magnetization of CoVG (a), NiVG (b), and FeGeG (c) at 4.2 °K.

temperature dependences of the specific heat at fields 5, 10, and 20 kOe agree fully with $C_{H=0}(T)$, beginning with field 30 kOe the maximum of the specific heat decreases in magnitude and shifts toward lower temperatures. Below $T \sim 5.2$ °K, the temperature dependence of the specific heat of CoVG in different fields does not differ from one to another.

Figure 19 shows the experimental field dependence of the magnetic moment at 4.2 °K for CoVG,[82] NiVG,[82] and FeGeG.[79] As is seen from the figure, a linear increase of magnetization continues until, at $H = H_E$, flipping of the magnetic moments of the sublattices occurs. The experimental values of H_E (see Table IV) agree well with those calculated in the molecular-field approximation.[67]

Measurements of the magnetic properties of MnGeG led to the supposition that there is a metamagnetic transition[57] in this garnet below T_N. Figure 20 shows the change of the magnetic moment of polycrystalline MnGeG at 4.2 °K. It is seen that the increase of the magnetic moment occurs smoothly; saturation, $M(0\,°\text{K}) = 2Ng\mu_B s = 44.6$ cgs emu/mol, is not attained up to $H \approx 300$ kOe.

Investigations of the specific heat of MnGeG in an external magnetic field[80] gave interesting results. As is seen from Fig. 21, already at $H = 5$ kOe the sharp maximum corresponding to antiferromagnetic ordering has shifted toward lower temperatures and become smaller in magnitude. At field $H = 10$ kOe, besides the antiferromagnetic maximum, which is shifted still more to the left and further broadened, there appears to the right of it a broad hump, which on further increase of the field remains almost unshifted with temperature but diminishes and broadens slightly. The maximum corresponding to the antiferromagnetic transition changes at $H = 20$ kOe to a step, which disappears at field 40 kOe. The slight difference in the $C_H(T)$ dependence at $T > 15$ °K is due to the fact that strong magnetic fields induce "magnetic order" when $T > T_N$.

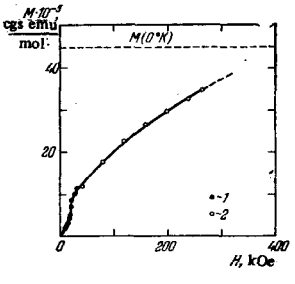

FIG. 20. Magnetization curve of MnGeG at 4.2 °K. 1, measurements in a superconducting solenoid; 2, measurements in pulsed magnetic fields.

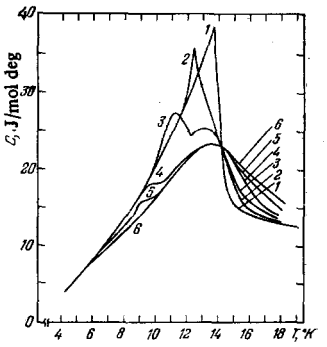

FIG. 21. Specific heat of MnGeG, H (kOe): 0 (1), 5 (2), 10 (3), 20 (4), 30 (5), 40 (6).

This behavior of the specific heat can be explained with the aid of the phase diagram shown in Fig. 22. It is assumed[60] that an external magnetic field induces in antiferromagnetic MnGeG a new magnetic structure (the intermediate phase "*MM*" in Fig. 25), whose stability is determined, of course, by competition of exchange interactions, anisotropy forces, the magnetic field, and temperature. Destruction of this phase corresponds to the broad hump on the $C_H(T)$ curves at $T \approx T_N$.

The shift of the antiferromagnetic maximum of the specific heat in an external field is determined by the phase boundary *AF–MM*. The results of magnetic measurements agree well with this transition line. As is seen from the phase diagram, the existence of an antiferromagnetic phase in MnGeG is bounded by magnetic field ~40 kOe, and a direct antiferromagnetism–paramagnetism transition is possible only in weak magnetic fields (0–7 kOe).

These characteristics of the antiferromagnetic ordering in MnGeG are obviously a necessary result of the existence in it of a Jahn–Teller effect (Mn^{3+} in octahedral groups is a Jahn–Teller ion[68]). In fact, it is only because of distortion of the body-centered lattice of the garnet that there could occur a strong anisotropy field (of the order of H_E) and a magnetic structure, with ferromagnetic chains, such that the exchange interaction within the chains is stronger than that between the chains. And this in turn produces the necessary conditions for a metamagnetic transition.

D. Antiferromagnetic resonance

Antiferromagnetic resonance (AFMR) in a spin-flop state ($H_0 > H_{sf}$) was discovered and investigated on monocrystals of FeGeG[87] and CrGeG.[86] Figure 23 shows the angular dependence of the resonance field (H_0) in planes (110), Curve 1, and (100), Curve 2, for a spherical specimen of FeGeG of diameter 1.2 mm. The fourfold symmetry of H_0 in plane (100) and the twofold in plane (110) indicate that FeGeG at 4.2 °K is an undis-

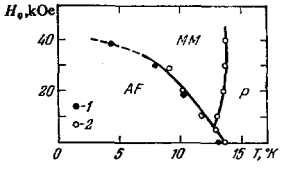

FIG. 22. Phase diagram of MnGeG according to data from: (1) magnetic measurements; (2) specific heat.

torted cubic antiferromagnet with directions of easy magnetization along axes ⟨111⟩; that is, the anisotropy constant $K_1 < 0$.

The experimental results (the points in Fig. 23) are described well by the formula (solid line)

$$\left(\frac{\omega}{\gamma}\right)^2 = H_0^2 + 3B(\theta, \varphi) H_E H_A + H_\Delta^2, \qquad (17)$$

which differs from the usual field dependence of the AFMR frequency of a cubic crystal,[89] for $H_0 > H_{sf}$, by the presence of an isotropic gap H_Δ^2. The angular dependence in (17) has the following form[89]:

$$B\left(\frac{\pi}{2}, \varphi\right) = -4\cos\sqrt{\frac{4\varphi}{7+\cos 4\varphi}}$$

for plane (100), and for resonance in plane (110)

$$B\left(\theta, \frac{\pi}{4}\right) = \begin{cases} -1 + \frac{13}{2}\cos^2\theta - 6\cos^4\theta & \text{for } \theta \text{ between [001] and [111]}, \\ \frac{(2-\sin^2\theta)(3\sin^2\theta - 1)}{2+\sin^2\theta} & \text{for } \theta \text{ between [111] and [110]}. \end{cases}$$

Here θ and φ are polar and azimuthal angles with the corresponding crystal axes. $H_\Delta^2 = H_{ms} H_E$ kOe^2 is apparently of magnetostrictive character (see note 3 added in proof, p. 165).

By using the experimental value $H_E = 404$ kOe,[79] one can estimate the magnetostriction and anisotropy fields for FeGeG:

$$H_{ms} \approx 3 \text{ kOe}, \quad H_A = 15.3 \text{ Oe}. \qquad (18)$$

The values found for H_A and H_Δ^2 give good agreement of the experimental results with the frequency dependence of AFMR along fixed crystallographic directions.[87]

Since $H_A = 4K_1/3g\mu_B s$, we get for the anisotropy constant $K_1 = -22.6 \cdot 10^{-4}$ cm^{-1}. This value may be compared with $K_1 = -10 \cdot 10^{-4}$ cm^{-1} obtained for the octahedral sublattice of $Y_3Fe_5O_{12}$ by the method of ferrimagnetic resonance.[90] It is obvious that this is single-ion anisotropy, whose basic mechanism for Fe^{3+} in the garnet structure is, according to Geschwind,[72] due to splitting of the s state in the cubic and trigonal crystalline fields. But if we use the corresponding crystalline field parameters determined from EPR of the Fe^{3+} ions in diamagnetic gallates and aluminates,[91] we get for FeGeG $K_1 = -72 \cdot 10^{-4}$ cm^{-1}, which exceeds by a factor of more than three the value found from AFMR. It is possible that the chief reason for this is the strong dependence of the crystalline field parameters on the degree of distortion of the octahedron surrounding the Fe^{3+}. FeGeG has a rather symmetric octahedron: the difference in the length of the edges does not exceed 0.1 Å, whereas, for example, for YGaG this value is 0.3 Å[92] (see note 4 added in proof, p. 165).

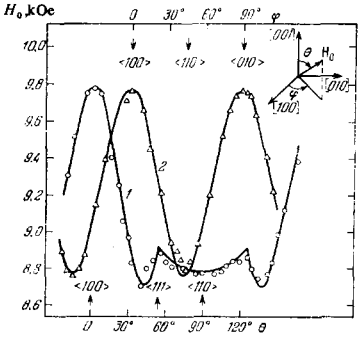

FIG. 23. Angular variation of AFMR field of FeGeG at 4.2 °K, for frequency 26.75 GHz. 1, (110) plane; 2, (100) plane.

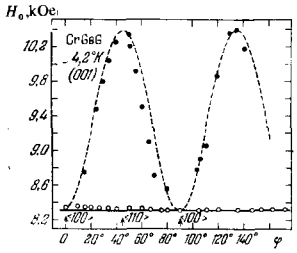

FIG. 24. Angular variation of AFMR field of CrGeG at 4.2 °K, for frequency 26.75 GHz, in (100) plane.

Results of AFMR measurements on CrGeG are given in Figs. 24 and 25. As is seen from these figures, the axis [100] is an axis of easy magnetization; that is, $K_1 > 0$. An interesting feature of CrGeG is the existence of a double resonance. In plane (001) (Fig. 24), the lower-field resonance is independent of angle. Analysis of the equilibrium spin configurations shows that this resonance is due to a sublattice magnetization directed along the easy axis [001]. This axis corresponds to an "absolute" minimum of the anisotropy energy and to an angular function in equation (17)

$$B\left(\frac{\pi}{2}, \varphi\right) \equiv B^{(m)} = -1.$$

The upper resonance corresponds to a sublattice magnetization perpendicular to axis [001]: a relative minimum of the anisotropy energy, with

$$B\left(\frac{\pi}{2}, \varphi\right) \equiv B^{(m')} = -\cos 4\varphi.$$

For $\phi = 0$ (or 90°), two degenerate minima occur, and a single resonance is observed. The solid and dotted lines in Fig. 24 correspond to $B^{(m)}$ and $B^{(m')}$ in the function (17), with the values

$$H_E H_A = 9.5 \text{ kOe}^2, \quad H_\Delta^2 = 3.4 \text{ kOe}^2.$$

By using the experimental value $H_E = 256$ kOe for CrGeG, we find $H_A = 35.8$ Oe and, correspondingly, $K_1 = 27.1 \cdot 10^{-4}$ cm^{-1} ($H_A = 2K_1/M_0$).

For plane (110), in the angle interval $0 \leq \theta \leq 54.7°$, there is a single resonance (Fig. 25), corresponding to

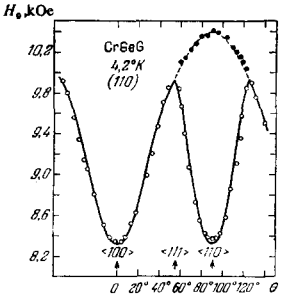

FIG. 25. Angular variation of AFMR field of CrGeG at 4.2 °K, for frequency 26.75 GHz, in (110) plane.

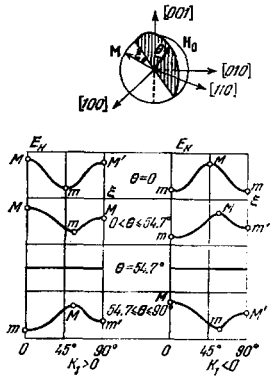

FIG. 26. Position of magnetic moment (M) and magnetic anisotropy energy (E_K) in the spin-flop plane, when the external field H_0 lies in a (110) plane.

a unique minimum of the energy with angular function

$$B\left(\theta, \frac{\pi}{4}\right)=\frac{2-7\cos^2\theta+9\cos^6\theta}{3-10\cos^2\theta+3\cos^4\theta}. \tag{19}$$

In the interval $54.7° \leq \theta \leq 90°$, a double resonance is observed, corresponding to

$$B^{(m)}=-1+\frac{13}{2}\cos^2\theta-6\cos^4\theta$$

and (20)

$$B^{(m')}=1-\frac{3}{2}\cos^2\theta.$$

The theoretical curves in Fig. 25 were calculated with the same parameters as for plane (100).

The physical nature of the peculiarities of AFMR in FeGeG and CrGeG can be explained, according to Eastman, Shafer, and Figat,[93] as follows.

For an external field $H_0 > H_{sf}$, the spin axis lies in the plane perpendicular to H_0; the magnetization is turned into the field direction through a small angle $H_0/2H_E$, and the position of M in the spin-flop plane is determined by the minimum of the anisotropy energy E_K (within the plane). For an H_0 lying in plane (110), this is illustrated by Fig. 26. When $0 \leq \theta \leq 54.7°$, with $K_1 > 0$, there are a single minimum of the anisotropy energy (m) and two maxima, an absolute (M) and a relative (M'). When $54.7° \leq \theta \leq 90°$, two minima of E_K appear: an absolute m (at $\xi = 0$) and a relative m' (at $\xi = 90°$) (ξ is the angle in the spin-flop plane).

An analogous situation will obviously exist also when $K_1 < 0$ in plane (001). In the angle interval $0° \leq \theta \leq 54.7°$ two resonances occur, corresponding to angles $\xi = 0$ and $\xi = 90°$, which are not always observed experimentally, perhaps because of the small intensity of the high-field resonance.

Thus investigation of AFMR in garnets enables us to obtain information about the equilibrium spin configurations, the anisotropy, and the magnetoelastic interactions in antiferromagnetic garnets. We note that in this connection static magnetic methods, for crystals with high symmetry, are apparently much less informative.

E. Rare-earth germanates $Ca_3R_2Ge_3O_{12}$

In the rare-earth germanates $M_3[R_2]Ge_3O_{12}$, where M is Ca^{2+} or Sr^{2+} and R is Dy^{3+}, Ho^{3+}, Er^{3+}, Tm^{3+} or Yb^{3+}, the R^{3+} ions occupy "extraordinary" coordination positions, octahedral a sites.[94] The lattice parameters of the garnets $Ca_3R_2Ge_3O_{12}$ (RGeG) exceed by about 0.3 Å the parameters of the corresponding gallates RGaG.

Measurements of the magnetic suceptibility of RGeG in the temperature interval 1.6–300 °K have shown that they remain paramagnetic down to helium temperatures.[95,96] We reported in[97] observations in dysprosium, holmium, and erbium germanates at 4.2 °K of gigantic (for paramagnets) magnetostrictive effects, caused by characteristics of the interaction of the orbital angular momentum of the R^{3+} with the crystalline field of the lattice.

Recently observations of RGeG have been extended to the temperature range down to 0.1 °K.[98] As is seen from Fig. 27, the temperature dependence of the magnetic susceptibility of ErGeG (Curve 1) reveals at $T = 0.34$ °K a sharp maximum due, obviously, to antiferromagnetic ordering of Er^{3+} in the octahedral sublattice. Above 2 °K the susceptibility of ErGeG follows the Curie–Weiss law with a temperature-independent contribution,

$$\chi(T)=\frac{C}{T-\Theta_p}+\alpha. \tag{21}$$

The constants that describe the $\chi(T)$ dependence are given in Table VII. Noticeable in ErGeG is the positive sign of θ_p, which is evidence of the important role of exchange interactions of second nearest neighbors in the magnetic structure of ErGeG.

DyGeG and YbGeG remain paramagnetic down to 0.1 °K (Fig. 27, Curves 2 and 4). The variation of susceptibility with temperature follows the Curie–Weiss law, and as in ErGeG a Van Vleck contribution is observed (see Table VII). Figure 28a shows isotherms of the magnetization of DyGeG. Since the magnetization of a simple paramagnet (per mol of DyGeG) can be written in the form

$$M(H, T)=2Ng\mu_B s' B_{s'}(x)+\alpha H, \tag{22}$$

where s' is the effective spin of the ground state of the Dy^{3+}, and where $B_{s'}(x)$ is Brillouin function with argu-

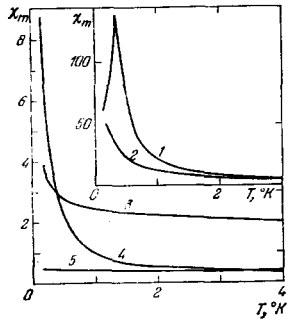

FIG. 27. Temperature dependence of the susceptibility of the garnet $Ca_3R_2Ge_3O_{12}$. $R = Er^{3+}$ (1), Dy^{3+} (2), Ho^{3+} (3), Yb^{3+} (4), and Tm^{3+} (5).

TABLE VII. Fundamental magnetic characteristics of garnets $Ca_3R_2Ge_3O_{12}$.

Specimen	Free-ion term	μ_{eff} of free ion, μ_B	μ_{eff}^{exp}, μ_B	C_m, cgs emu/mol	Θ_p, °K	α, $\frac{cgs\ emu}{mol}$	T_N, °K	$M_0 \cdot 10^{-3}$/mol
DyGeG	$^6H_{15/2}$	10.64	8.5	17.8	−0.3 °K	0.24	—	46
HoGeG	$^8I_5$	10.6	1.5	0.56	−0.13	1.94	—	1
ErGeG	$^4I_{15/2}$	9.58	8.1	16.5	+0.2	0.24	0.34	49
TmGeG	$^3H_6$	7.56	—	—	—	0.40	—	—
YbGeG	$^2F_{7/2}$	4.53	2.15	1.16	0	0.024	—	15

ment $x = g\mu_B s'H/kT$, extrapolation of the linear part of the $M(H, T)$ curve to $H = 0$ makes it possible to find M_0 (see Table VII) and α. By use of the values thus found for M_0, x, and α, the variation of $[M(H, T) - \alpha H]/M_0$ with x has been plotted in Fig. 28b for temperatures 1.6, 3.1, and 4.2 (points). The solid line in Fig. 28b shows the Brillouin function for spin $s = \frac{1}{2}$. It is seen that the experimental points lie on a single curve and follow the theoretical variation quite well. This enables us to conclude that the lowest state of Dy^{3+} in octahedral sites, as in the case of DyAlG, is a doublet.

In TmGeG and HoGeG no magnetic ordering is observed (Curves 3 and 5 in Fig. 27). The susceptibility of TmGeG is independent of temperature over the range 0.1–4.2 °K; that is, the lowest state of Tm^{3+} in the octahedral crystalline field of the garnet is obviously a singlet, and the excited states lie considerably higher. The susceptibility of TmGeG is well described by the function (21) with a relatively large value of α. Unexpected is the strong temperature dependence of the susceptibility of HoGeG, since the lowest state of Ho^{3+}, on the assumption of a cubic crystalline field, is a nonmagnetic level.[99]

4. MAGNETIC ORDER OF Fe^{3+} IONS IN TETRAHEDRA

In contrast to the a sublattice, the tetrahedral sites in the garnet structure may be occupied only by Fe^{3+} ions. Table VIII shows the magnetic characteristics of six polycrystalline specimens with Fe^{3+} in tetrahedra and with various nonmagnetic ions in the a and c sublattices. In the case of garnet VI, a small amount of Ga^{3+} has been introduced into the d sublattice, since the garnet $YCa_2Zr_2Fe_3O_{12}$ does not form. The values of T_N determined from the temperature dependence of the Mössbauer spectra,[106] as is seen from Table VIII, are correlated with the variation of the lattice parameter a_0. This dependence is quite strong: an increase of a_0 by 0.075 Å leads to a decrease of T_N by 20 °K. It is interesting to note that measurements of the magnetic susceptibility and of the temperature dependence of Young's modulus (E) of specimens I–V did not permit determination of their Néel temperature[101] (Fig. 29). The $\chi^{-1}(T)$ dependences of these garnets at $T > 100$ °K follow the Curie–Weiss law with the values of the paramagnetic Curie temperature Θ_p shown in Table VIII, and $E(T)$ displays no noticeable irregularity near T_N, as is observed in the case of garnets with octahedral $3d$ ions.[57]

TABLE VIII. Lattice parameters and magnetic characteristics of garnets with Fe^{3+} in tetrahedra.[100-103]

Garnet	a_0, Å	T_N, °K	$-\Theta_p$, °K	$-J_1$, °K	$-J_2$, °K
I. $Na_3[Te_2](Fe_3)O_{12}$	12.524	67	300	4.7—5.5	2.5—2.9
II. $NaCa_2[Sb_2](Fe_3)O_{12}$	12.600	47	190	2.7—3.7	1.6—2.6
III. $Ca_3[SnSb](Fe_3)O_{12}$	12.634	40	136	1.6—3.0	1.0—1.7
IV. $GdCa_2[Sn_2](Fe_3)O_{12}$	12.666	34.5	64	—	—
V. $Ca_3[ZrSb](Fe_3)O_{12}$	12.669	11 (?)	120	—	—
VI. $YCa_2[Zr_2](Fe_{2.75}Ga_{0.25})O_{12}$	12.68	7	40	0.59—0.65	0.30—0.34

Recently[101,102] detailed neutron-diffraction investigations were undertaken in garnets with Fe^{3+} in tetrahedra. The specimens studied were those shown in Table VIII, with the exception of IV, which contains gadolinium in the dodecahedra. On the basis of the neutron-diffraction data the crystal structure was refined, the exchange bonds between magnetic ions in the d sublattice were analyzed (the interatomic distances and the valence angles were calculated for each bond), and the magnetic structures were determined. It was established that in all the garnets investigated except $Ca_3ZrSbFe_3O_{12}$, in which long-range magnetic order is absent, antiferromagnetic ordering of the Fe^{3+} ions occurs at low temperatures, with various triangular configurations of the spins. The magnetic structures (Fig. 30) of garnets I, II, and III differ in the orientation of the spins with respect to the crystallographic axes and are described by

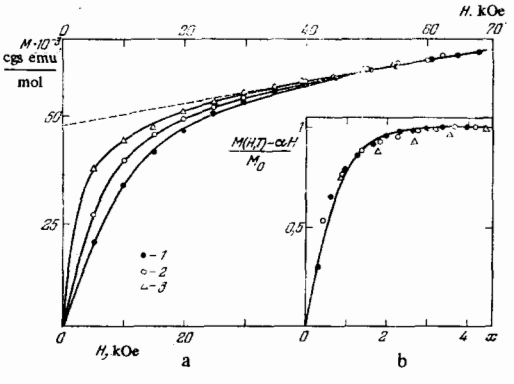

FIG. 28. a, Magnetization isotherms of $Ca_3Dy_2Ge_3O_{12}$. b, Variation of relative magnetization with $x = g\mu_B sH/kT$. 1, 4.2 °K; 2, 3 °K; 3, 1.6 °K.

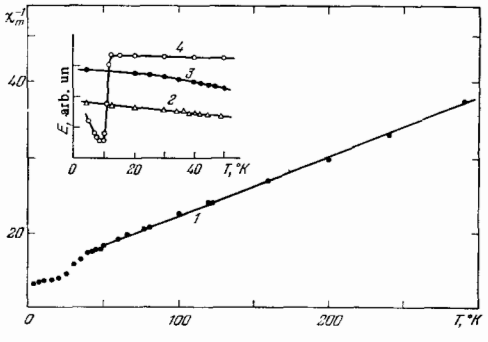

FIG. 29. Temperature dependence of inverse molar susceptibility (1) and Young's modulus (2), for garnet $NaCa_2[Sb_2](Fe_3)O_{12}$, $Ca_3[SnSb](Fe_3)O_{12}$ (3), and $Ca_3[Fe_2]Ge_3O_{12}$ (4).

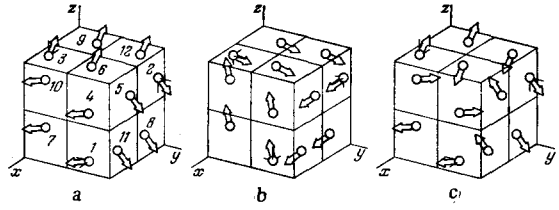

FIG. 30. Magnetic structures of garnets I (a), II and III (b), and VI (c). (Notation in accordance with Table VIII.)

Shubnikov group $R\bar{3}'$. The magnetic structure of garnet VI belongs to Shubnikov group $R\bar{3}'$.

The magnetic structure of garnet I is shown in Fig. 30a, which shows the directions of the magnetic moments of twelve atoms that form a space-centered Bravais lattice. The magnetic moments of the remaining atoms are obtained by simple translations 1/2, 1/2, 1/2. The spins of all the atoms in this garnet are directed along a [110] axis to within accuracy 0.7°. The magnetic structure of garnets II and III is shown in Fig. 30b. The spin directions in these garnets are close to a $[\bar{1}12]$ axis. For garnet VI the spins of the 24 iron atoms contained in an elementary cell form three antiferromagnetic sublattices, turned one with respect to another through an angle 120° (Fig. 30c), and the spins of all the atoms, to within accuracy 5°, lie along one of the [110] axes.

The exchange-interaction parameters obtained in[102] for garnets with Fe^{3+} in the *d* sublattice (Table VIII), and also comparison of them with the geometrical characteristics of the corresponding exchange bonds, enabled the authors[102] to conclude that interactions between Fe^{3+} ions with the participation of a diamagnetic cation (*D*) from an octahedral site and of two oxygen ions (Fe^{3+}–O^{2-}–D–O^{2-}–Fe^{3+}) are dominant. Their energy considerably exceeds the energy of interaction with the participation only of two intermediate oxygen ions (Fe^{3+}–O^{2-}–O^{2-}–Fe^{3+}). This result is quite unexpected and obviously requires explanation, not only from the point of view of the geometry of the bonds, but also in the language of molecular orbitals.

5. CONCLUSION

On the basis of the existing experimental data, we shall now note several, in our opinion the most important and interesting, properties that enable us to distinguish antiferromagnetic garnets among the quite numerous class of magnetically ordered dielectrics.

1. These compounds are exceptionally suitable objects for test of various models in the theory of magnetism and for study of magnetic phase transitions. Garnets withhighly anisotropic rare-earth ions are Ising antiferromagnets, while the properties of garnets with 3*d* ions are well described by the Heisenberg model of exchange interaction.

2. The exactness of stoichiometric composition of garnets distinguishes them favorably from other oxide compounds (for example spinels and perovskites), which easily form defect structures. This fact, in combination with experimentally convenient Néel points, makes it possible to use antiferromagnetic garnets to obtain quantitative data on magnetic phase transitions both of the first and of the second kind. Especially interesting is study of the physical properties in the neighborhood of tricritical points: in particular, in a scheme of comparison with the tricritical behavior of an He^3He^4 mixture, for which good agreement with theory is observed.

3. The characteristics of the garnet structure make it possible to introduce the same magnetic ions into different crystallographic positions and thus to investigate the effects of crystalline fields of different symmetry in antiferromagnets. There exists a sufficiently numerous set of 3*d* and 4*f* ions to make possible the study of such phenomena as "two-singlet magnetism," the Jahn–Teller effect, nuclear antiferromagnetism, etc.

4. The comparatively small exchange field (~ 100 kOe) and low anisotropy (~ 10 Oe) of antiferromagnetic garnets create a unique opportunity for experimental investigation of phase transitions induced by an external magentic field, Apparently it is in principle possible to produce garnets in which a transition from the antiferromagnetic to the ferrimagnetic state will be observed in fields of the order of several tens of kilo-oersteds.

5. It must be noted that understanding of the mechanism of exchange interactions in compounds with the garnet structure still remains very far from completeness. In order to obtain a clear picture of the indirect exchange interaction that occurs in garnets through two or even three intermediate links (two oxygen ions and a nonmagnetic cation), we need an analysis of the possible spin configurations that takes account of the interactions of the atoms of all the Bravais lattices and of the geometric characteristics (interatomic distances and valence angles). In this respect the greatest information can apparently be obtained from neutron-diffraction investigations of antiferromagnetic garnets.

6. At present the properties of compounds with the garnet structure are most often considered with a view to their practical use. Already the range of application of garnets is exceptionally broad: from materials for optical quantum generators to numerous devices in channels for the processing of microwave signals. In recent years new possibilities have opened up for use of iron garnets (in the form of monocrystalline films) as materials with cylindrical domains for production of fast-acting memory elements of large capacity. At present it is apparently too early to speak of concrete application of antiferromagnetic garnets. But the low magnetocrystalline anisotropy of these compounds, the optical properties near the infrared region,[104] and specific metamagnetic transitions are stimulating the further development of research in the investigation of antiferromagnetic garnets as new magnetic materials.

Note added in proof. 1 (To p. 156). X-ray investigations of MnGeG in the temperature interval 4.2–300°K[105] have established in this compound a tetrahedral distortion of the structure, produced by a cooperative Jahn–Teller effect.

2 (To p. 156). In[106] the spin-wave contribution to the specific heat of MnVG has been derived. The value of the exchange interaction in the spin-wave approximation agrees well with the corresponding values given by the molecular-field method.

3 (To p. 161). Calculation of the AFMR spectrum of a cubic antiferromagnet with allowance for magnetoelastic interaction[107] has shown that H_Δ^2 has an anisotropic part; the angular dependence of H_Δ^2 is in general different from the angular dependence of the anisotropic gap due to K_1.

4 (To p. 161). The parameters of the spin Hamiltonian for FeGeG determined by the EPR method[108] give, at 4.2 °K, $K_1 \approx 65 \cdot 10^{-4}$ cm^{-1}. For quantitative agreement of the AFMR and EPR data, it is apparently necessary to take account of the second anisotropy constant (K_2).

[1]L. Néel, Ann. Phys. (Paris) 18, 5 (1932).
[2]L. Landau, Phys. Z. Sowjetunion 4, 675 (1933).
[3]S. V. Vonsovskiĭ, Magnetizm (Magnetism), M., "Nauka", 1971.
[4]A. S. Borovik-Romanov, Antiferromagnetizm (Antiferromagnetism), Series "Itogi nauki" (Results of Science), Fizmatem. nauki. (Physical-Mathematical Sciences) 4, M., VINITI, 1962.
[5]V. V. Eremenko, Vvedenie v opticheskyuy spektroskopiyu magnetikov (Introduction to the Optical Spectroscopy of Magnetic Materials), Kiev, Naukova dumka, 1975.
[6]A. S. Gurevich, Magnitnyĭ rezonans v ferritakh i antiferromagnetikakh (Magnetic Resonance in Ferrites and Antiferromagnets), M., Nauka, 1973.
[7]G. A. Smolenskiĭ, V. V. Lemanov, G. M. Nedlin, M. P. Petrov, and R. V. Pisarev, Fizika magnitnykh dielektrikov (Physics of Magnetic Dielectrics), L., Nauka, LO., 1974.
[8]L. Néel, C. R. Acad. Sci. (Paris) 239, 8 (1954).
[9]R. Pauthenet, J. Phys. Radium 20, 388 (1959).
[10]D. Boakes, G. Garton, D. Ryan, and W. P. Wolf, Proc. Phys. Soc. Lond. 74, 663 (1959).
[11]R. M. Bozorth and S. Geller, J. Phys. Chem. Solids 11, 263 (1959).
[12]S. Geller, R. M. Bozorth, M. A. Gilleo, and C. E. Miller, J. Phys. Chem. Solids 12, 111 (1959).
[13]W. P. Wolf, M. Ball, T. Hutchings, M. J. M. Leask, and A. F. G. Wyatt, J. Phys. Soc. Jap. 17, Suppl. B-1, 443 (1962).
[14]M. Ball, G. Garton, M. J. M. Leask, D. Ryan, and W. P. Wolf, J. Appl. Phys. 32, 267S (1961).
[15]A. H. Cooke, T. L. Thorp, and M. R. Wells, Proc. Phys. Soc. Lond. 92, 400 (1967).
[16]D. G. Onn, H. Meyer, and J. P. Remeika, Phys. Rev. 156, 663 (1967).
[17]A. Herpin and P. Mériel, C. R. Acad. Sci. (Paris) 259, 2416 (1964).
[18]F. Bertaut and F. Forrat, C. R. Acad. Sci. (Paris) 243, 1219 (1956).
[19]M. Ball, W. P. Wolf, and A. F. G. Wyatt, Phys. Lett. 10, 7 (1964).
[20]M. J. Filippi, C. R. Acad. Sci. B 273, 72 (1972).
[21]J. P. Redoules, P. Carrara, A. R. Fert, M. C. Lanusse, and G. Mischler, J. Phys. (Paris) 33, 281 (1972).
[22]A. Gavignet-Tillard, J. Rammann, and L. De Seze, J. Phys. (Paris) 34, 27 (1973).
[23]A. Gavignet-Tillard, J. Hammann, and L. De Seze, Proc. Internatl. Conf. Magnetism (ICM-73), Vol. 1, M., Nauka, 1974, p. 374.
[24]J. Hammann and P. Manneville, in: Low Temperature Physics LT-13, Vol. 2, Plenum Press, New York-London (1974), p. 328.
[25]J. Hammann and P. Manneville, J. Phys. (Paris) 34, 615 (1973).
[26]H. W. Capel, Physica 31, 1152 (1965).
[27]R. Bidaux, P. Carrara, and B. Vivet, J. Phys. (Paris) 29, 357 (1968).
[28]B. Schneider, D. P. Landau, B. E. Keen, and W. P. Wolf, Phys. Lett. 23, 210 (1966).
[29]J. A. Koningstein and G. Schaack, Phys. Rev. B2, 1242 (1970).
[30]P. Bidaux, A. Gavignet-Tillard, and J. Hammann, J. Phys. (Paris) 34, 19 (1973).
[31]R. Bidaux and B. Vivet, J. Phys. (Paris) 29, 57 (1968).
[32]M. Ball, M. J. M. Leask, W. P. Wolf, and A. F. G. Wyatt, J. Appl. Phys. 34, 1104 (1963).
[33]D. P. Landau, B. E. Keen, B. Schneider, and W. P. Wolf, Phys. Rev. B3, 2310 (1971).
[34]G. F. Tuthill, F. Harbus, and H. E. Stanley, Phys. Rev. Lett. 31, 527 (1973).
[35]D. R. Nelson and J. Rudnick, Phys. Rev. Lett. 35, 178 (1975).
[36]V. J. Emery, Phys. Rev. B11, 3397 (1975).
[37]J. C. Norvell, W. P. Wolf, L. M. Corliss, J. M. Hastings, and R. Nathans, Phys. Rev. 186, 557 (1969).
[38]A. T. Skjeltorp, R. Alben, and W. P. Wolf, AIP Conf. Proc. 18, Part 2, 770 (1974).
[39]N. Girodano and W. P. Wolf, Phys. Rev. Lett. 35, 799 (1975).
[40]J. F. Dillon, E. Yi Chen, and W. P. Wolf, reference,[23] p. 38.
[41]J. F. Dillon, Jr., E. Yi Chen, N. Girodano, and W. P. Wolf, Phys. Rev. Lett. 33, 98 (1974).
[42]M. Blume, L. M. Corliss, J. M. Hastings, and E. Schiller, Phys. Rev. Lett. 32, 544 (1974).
[43]R. Alben, M. Blume, L. M. Corliss, and J. M. Hastings, Phys. Rev. B11, 295 (1975).
[44]W. P. Wolf, AIP Conf. Proc. 24, 255 (1975).
[45]B. E. Keen, D. P. Landau, and W. P. Wolf, Phys. Lett. 23, 202 (1966).
[46]W. Prandl, Z. Kristallogr. 134, 333 and 344 (1971).
[47]I. S. Lyubutin and A. P. Dodokin, Kristallografiya 15, 1249 (1971) [Sov. Phys. Crystallogr. 15, 1091 (1971)].
[48]A. P. Dodokin, I. S. Lyubutin, L. M. Belyaev, and V. P. Peshkov, Zh. Eksp. Teor. Fiz. 63, 1393 (1972) [Sov. Phys. JETP 36, 738 (1973)].
[49]W. Prandl, Phys. Status Solidi (b) 55, K159 (1973).
[50]R. Plumier, Solid State Commun. 12, 109 (1973).
[51]T. V. Valyanskaya, V. P. Plakhtiĭ, and V. I. Sokolov, Zh. Eksp. Teor. Fiz. 70, 2279 (1976) [Sov. Phys. JETP 43, 1189 (1976)].
[52]B. V. Mill', in: Magnitnye i kristallograficheskie issledovaniya ferritov (Magnetic and Crystallographic Investigations of Ferrites), M., Izd-vo Mosk. un-ta, 1971, p. 56.
[53]S. Geller, Z. Kristallogr. 125, 1 (1967).
[54]B. V. Mill' and G. Ronniger, in: Fizika i khimiya ferritov (Physics and Chemistry of Ferrites), M., Izd-vo Mosk, un-ta, 1973, p. 98.
[55]L. M. Belyaev, I. S. Lyubutin, B. V. Mill', and V. A. Povitskiĭ, Fiz. Tverd. Tela (Leningrad) 11, 795 (1969) [Sov. Phys. Solid State 11, 644 (1969)].
[56]E. L. Dukhovskaya and B. V. Mill', Kristallografiya 19, 84 (1974) [Sov Phys. Crystallogr. 19, 47 (1974)].
[57]K. P. Belov, B. V. Mill', G. Ronniger, V. I. Sokolov, and T. D. Hien, Fiz. Tverd. Tela (Leningrad) 12, 1761 (1970) [Sov. Phys. Solid State 12, 1393 (1970)].
[58]G. Ronniger, B. V. Mill', and V. I. Sokolov, Kristallografiya 19, 361 (1974) [Sov. Phys. Crystallogr. 19, 219 (1974)].
[59]I. V. Golosovsky, V. P. Plakhty, B. V. Mill, V. I. Sokolov, and O. P. Shevaleevskii, Solid State Commun. 14, 309 (1974).

[60]R. Plumier, Solid State Commun. 10, 5 (1972).
[61]V. P. Plakhtiĭ, I. V. Golosovskiĭ, V. A. Kudrashev, and O. P. Smirnov, Pis'ma Zh. Eksp. Teor. Fiz. 16, 276 (1972) [JETP Lett. 16, 194 (1972)].
[62]R. P. Ozerov and N. V. Fadeeva, Pis'ma Zh. Eksp. Teor. Fiz. 16, 282 (1972) [JETP Lett. 16, 198 (1972)].
[63]R. Plumier, Solid State Commun. 9, 1723 (1971).
[64]W. Prandl, Solid State Commun. 10, 529 (1972).
[65]J. S. Smart, Effective Field Theories of Magnetism, W. B. Saunders Co., Philadelphia-London, 1966 (Russ. transl., M., Mir, 1968).
[66]V. P. Palkhtiĭ, Author's abstract, candidate's dissertation, L., LIYaF, 1973.
[67]L. G. Mamsurova, Author's abstract, candidate's dissertation, M., MGU, 1975.
[68]A. Abragam and B. Bleaney, Electron Paramagnetic Resonanc of Transition Ions, Oxford, 1970 (Russ. transl., M., Mir. 1973, Vol. 2).
[69]V. P. Plakhtiĭ and I. V. Golosovskiĭ, Fiz. Tverd. Tela (Leningrad) 14, 2760 (1972) [Sov. Phys. Solid State 14, 2387 (1973)].
[70]H. Saji, Y. Hanayama, T. Yamagaya, and M. Asanuma, Phys. Lett. A34, 349 (1971).
[71]A. Abragam and M. H. L. Pryce, Proc. R. Soc. Lond. A205, 135 (1951).
[72]S. Geschwind, Phys. Rev. 121, 363 (1961).
[73]V. I. Sokolov, H. Szymczak, and W. Wardzyński, Phys. Status Solidi (b) 55, 781 (1973).
[74]J. R. Chamberlain and R. W. Cooper, Proc. Phys. Soc. Lond. 87, 967 (1966).
[75]P. Novak and V. Havlíček, Czech. J. Phys. 26, 4 (1976).
[76]M. D. Sturge, F. R. Merritt, J. C. Hensel, and J. P. Remeika, Phys. Rev. 180, 402 (1969).
[77]V. Havlíček and P. Novák, Czech. J. Phys. 24, 188 (1974).
[78]L. G. Mamsurova and V. I. Sokolov, Summaries of reports of All-Union Conference on Low-Temperature Physics, Donetsk, 1972, p. 195.
[79]Y. Allain and M. Lecomte, Solid State Commun. 14, 119 (1974).
[80]K. P. Belov, T. V. Valyanskaya, L. G. Mamsurova, and V. I. Sokolov, Zh. Eksp. Teor. Fiz. 65, 1133 (1973) [Sov. Phys. JETP 38, 561 (1974)].
[81]L. G. Mamsurova and E. M. Speranskaya, Fiz. Tverd. Tela (Leningrad) 16, 3603 (1974) [Sov. Phys. Solid State 16, 2342 (1975)].
[82]L. G. Mamsurova, V. I. Sokolov, and E. M. Speranskaya, Zh. Eksp. Teor. Fiz. 69, 666 (1975) [Sov. Phys. JETP 42, 338 (1975)].
[83]T. V. Valyanskaya, B. V. Mill'. and V. I. Sokolov, Fiz. Tverd. Tela (Leningrad) 18, 1212 (1976) [Sov. Phys. Solid State 18, 696 (1976)].
[84]C. Domb and N. W. Dalton, Proc. Phys. Soc. Lond. 89, 859 and 873 (1966).
[85]C. Domb and A. R. Miedema. in: Progress in Low Temperature Physics (C. J. Gorter, ed.), Vol. 4, North-Holland, 1964, p. 296.
[86]N. W. Dalton and D. W. Wood, Proc. Phys. Soc. Lond. 90, 459 (1967).
[87]K. P. Belov, B. V. Mill', V. I. Sokolov, and O. I. Shevaleevskiĭ, Pis'ma Zh. Eksp. Teor. Fiz. 20, 98 (1974) [JETP Lett. 20, 42 (1974)].
[88]T V. Valyanskaya, B. V. Mill', V. I. Sokolov, and O. I. Shevaleevskiĭ, Summaries of reports of All-Union Conference on the Physics of Magnetic Phenomena, Baku, 1975, p. 89.
[89]D. T. Teaney, M. J. Freiser, and R. W. H. Stevenson, Phys. Rev. Lett. 9, 912 (1962).
[90]G. P. Rodrigue, H. Meyer, and R. V. Jones, J. Appl. Phys. 31, 376S (1960).
[91]L. Rimai and T. Kushida, Phys. Rev. 143, 160 (1966).
[92]F. Euler and J. A. Bruce, Acta Crystallogr. 19, 971 (1965).
[93]D. E. Eastman, M. W. Shafer, and R. A. Figat, J. Appl. Phys. 38, 5209 (1967).
[94]B. V. Mill', Dokl. Akad. Nauk SSSR 165, 555 (1965) [Sov. Phys. Dokl. 10, 1015 (1966)].
[95]K. P. Belov, R. V. Mill', V. I. Sokolov, and T. D. Hien, Fiz. Met. Metalloved. 27, 610 (1969) [Phys. Met. Metallogr. 27, No. 4, 38 (1969)].
[96]L. Suchow and M. Kokta, J. Solid State Chem. 5, 85 (1972).
[97]K. P. Belov, V. I. Sokolov, and T. D. Hien, Fiz. Tverd. Tela (Leningrad) 10, 3706 (1968) [Sov. Phys. Solid State 10, 2946 (1969)].
[98]T. V. Valyanskaya and V. I. Sokolov, Fiz. Tverd. Tela (Leningrad) 18, 297 (1976) [Sov. Phys. Solid State 18, 175 (1976)].
[99]K. R. Lea, M. J. Leask, and W. P. Wolf, J. Phys. Chem. Solids 23, 1381 (1962).
[100]A. P. Dodokin, I. S. Lyubutin, B. V. Mill', and V. P. Peshkov, Zh. Eksp. Teor. Fiz. 63, 1002 (1972) [Sov. Phys. JETP 36, 526 (1973)].
[101]V. P. Plakhtii, I. V. Golosovskiĭ, M. N. Bedrizova, O. P. Smirnov, B. V. Mill'. V. I. Sokolov, and N. N. Parfenova, reference,[88] p. 145.
[102]V. P. Plakhtii, I. V. Golosovskiĭ, M. N. Bedrizova, O. P. Smirnov, B. V. Mill', V. I. Sokolov, and N. N. Parfenova, Preprint LIYaF Akad. Nauk SSSR No. 240, Leningrad, 1976.
[103]V. P. Plakhtii and I. V. Golosovskii, Phys. Status Solidi (b) 53, K37 (1972).
[104]D. J. Dentz, R. C. Puttbach, and R. F. Bellt, AIP Conf. Proc. 18, Part 2, 954 (1974).
[105]Z. A. Kazeĭ, B. V. Mill'. and V. I. Sokolov, Pis'ma Zh. Eksp. Teor. Fiz. 24, 229 (1976) [JETP Lett. 24, 203 (1976)].
[106]T. V. Valyanskaya and V. I. Sokolov, Fiz. Tverd. Tela (Leningrad) 18, 3718 (1976) [Sov. Phys. Solid State 18, 2168 (1976)].
[107]A. G. Berezin, V. I. Sokolov, V. G. Shavrov, and O. P. Shevaleevskiĭ, Summaries of reports of All-Union Conference on Low-Temperature Physics, Minsk, 1976, p. 643.
[108]P. Novák, V. Havlíček, B. V. Mill, V. I. Sokolov, and O. I. Shevaleevskii, Solid State Commun. 19, 631 (1976).

Translated by W. F. Brown, Jr.